INTERNATIONAL ATOMIC ENERGY AGENCY
UNITED NATIONS EDUCATIONAL, SCIENTIFIC AND CULTURAL ORGANIZATION

INTERNATIONAL CENTRE FOR THEORETICAL PHYSICS
34100 TRIESTE (ITALY) - P.O.B. 586 - MIRAMARE - STRADA COSTIERA 11 - TELEPHONES: 224281/2/3/4/5/6
CABLE: CENTRATOM - TELEX 460392-I

SMR/115 - 1

WINTER COLLEGE ON LASERS, ATOMIC AND MOLECULAR PHYSICS

(21 January - 22 March 1985)

Lecture 1: Topics in the Physics of Particle Accelerators.

A Storage-Ring FEL for the VUV.

A.M. SESSLER
Lawrence Berkeley Laboratory
University of California
Berkeley, California 94720
U.S.A.

TOPICS IN THE PHYSICS OF PARTICLE ACCELERATORS

Andrew M. Sessler

Lawrence Berkeley Laboratory
University of California
Berkeley, CA 94720

I. INTRODUCTION

High energy physics, perhaps more than any other branch of science, is driven by technology. It is not the development of theory, or consideration of what measurements to make, which are the driving elements in our science. Rather it is the development of new technology which is the pacing item.

Thus it is the development of new techniques, new computers, and new materials which allows one to develop new detectors and new particle-handling devices. It is the latter, the accelerators, which are at the heart of the science.

Without particle accelerators there would be, essentially, no high energy physics. In fact, the advances in high energy physics can be directly tied to the advances in particle accelerators. Looking terribly briefly, and restricting one's self to recent history, the Bevatron made possible the discovery of the anti-proton and many of the resonances, on the AGS was found the μ-neutrino, the J-particle and time reversal non-invariance, on Spear was found the ψ-particle, and, within the last year the Z_0 and $W^{\pm}$ were seen on the CERN SPS p-$\bar{p}$ collider. Of course one could, and should, go on in much more detail with this survey, but I think there is no need. It is clear that as better acceleration techniques were developed more and more powerful machines were built which, as a result, allowed high energy physics to advance.

What are these techniques? They are very sophisticated and ever-developing. The science is very extensive and many individuals devote their whole lives to accelerator physics. As high energy experimental physicists your professional lives will be dominated by the performance of "the machine"; i.e. the accelerator. Primarily you will be frustrated by the fact that it doesn't perform better. Why not?

In these lectures, six in all, you should receive some appreciation of accelerator physics. We cannot, nor do we attempt, to make you into accelerator physicists, but we do hope to give you some insight into

the machines with which you will be involved in the years to come. Perhaps, we can even turn your frustration with the inadequacy of these machines into marvel at the performance of the accelerators. At the least, we hope to convince you that the accelerators are central, not peripheral, to our science and that the physics of such machines is both fascinating and sophisticated.

The plan is the following: First I will give two lectures on basic accelerator physics; then you will hear two lectures on the state of the art, present limitations, the specific parameters of LEP, HERA, TEV2 and SLC, and some extrapolation to the next generation of machines such as the Large Hadron Collider (LHC), Superconducting Super Collider (SSC), and Large Linear Colliders; finally, I will give two lectures on new acceleration methods.

On basic accelerator physics (which material is encompassed by this article) I must, clearly, select some topics. Notice that everyone of the machines mentioned in the last paragraph is a colliding-beam device. The day of fixed-target machines, for high energy physics, seems over! My choice of topics, and emphasis, will be made with this trend very much in mind. In addition, I shall not go into anything in sufficient detail to allow you to go out and design an accelerator, but I do plan to present the basic physics and, thus, hopefully, give you some appreciation of the limits and performance capabilities of colliders. Lastly, I shall cover some topics where discrete particle effects are dominant, such as in stochastic cooling.

The plan of topics is to first cover single particle dynamics. A complete understanding of single particles is possible, and essential, to the design of particle-handling devices. We can, conveniently, break this up into transverse motion and longitudinal motion. Then I shall cover some topics in collective effects. These effects can be treated by perturbation theory (on the single particle motion), but one must note that it is the collective phenomena which produce the limits on performance and, hence, that it is a proper understanding of this perturbation theory which becomes the essence of accelerator physics. Lastly, I shall cover some topics where discrete particle effects are dominant, such as in stochastic cooling.

There is much material on particle accelerators for this is, after all, an art which is half-a-century old. The student might do well to firstly, consult the five general references listed here.[1,2,3,4,5] These books then give references to original papers and other books. The interested person will want to study the proceedings of the International Conferences on High Energy Accelerators (there have been 12 of them going back to 1956) and the many proceedings of the National Accelerator Conferences. (Published as special volumes, by the IEEE Trans. on Nuclear Science.)

Finally, by way of introduction, I shall not be elegant in my treatment. Rather than presenting Hamiltonians and formalism, I shall give the simplest approach which is adequate. Sometimes, this means using a physical argument, or simply stating, that one can ignore one thing or another. The doubtful reader, or the reader wishing a better treatment, is invited to read the literature where he probably will find what he desires.

PART A: SINGLE PARTICLE DYNAMICS

II. TRANSVERSE MOTION: LINEAR ANALYSIS

In analyzing the transverse motion it is convenient to break this up into linear and non-linear effects. The linear approximation, i.e. linear in the amplitudes of oscillation about a reference orbit, is an exceedingly good approximation and serves to give one a great deal of insight into particle motion in an accelerator. For this reason, the linear theory has been highly developed and is, by now, quite sophisticated. Furthermore, some very comprehensive computer programs have been developed and are now used, throughout the world, to quickly perform linear design of devices.

2.1 Equations of Motion

Everyone knows that in a homogeneous magnetic field B, a charged particle moves in a circle of radius ρ where

$$\rho = \frac{p}{eB} \quad , \tag{2.1}$$

where p is the momentum of the particles. The angular frequency of the particle, its cyclotron frequency, is

$$\omega_c = \frac{eB}{m\gamma} \quad . \tag{2.2}$$

where $\gamma = (1 - \beta^2)^{-1/2}$ is the relativistic factor and β is its velocity in units of the velocity of light.

A convenient set of units is

$$\rho(m) = \frac{p(GeV/c)}{(0.3)B\ (T)} \quad . \tag{2.3}$$

The first circular accelerator, the cyclotron, was based upon the observation that for a non-relativistic particle ω_c is a constant and hence that fixed frequency radio frequency could be employed to accelerate these particles.

A modern accelerator, again as everyone knows, does not, at all subject the particles to a constant field. In a general magnetic field there exists a "closed orbit," or periodic solution of the equations of motion. This orbit is usually planar and transverse motion in this plane is described by the displacement x. Vertical motion (i.e. perpendicular to the median, equilibrium, plane) is described by the displacement y.

From the Lorentz force or, more elegantly, from the Hamiltonian for a particle in a static (but spacially varying) magnetic field one obtains (keeping only linear terms):

$$\frac{d^2x}{ds^2} + \left[\frac{1}{\rho^2(s)} - k(s)\right] x = \frac{1}{\rho(s)} \frac{\Delta p}{p} \quad ,$$

$$\frac{d^2y}{ds^2} + k(s)y = 0 \quad . \tag{2.4}$$

The arc length along the equilibrium orbit is s, ρ(s) is the radius of curvature of this orbit, and k(s) which describes the focusing property of the magnetic field is given by

$$k(s) = -\frac{1}{B\rho} \frac{\partial B_y}{\partial x} \quad . \tag{2,5}$$

From Eq. (2.1) one sees that Bρ, the "magnetic rigidity" is just the momentum of a particle and, of course, a constant in a static magnetic field. The "momentum error" (i.e. from that of the "particle" which defines the equilibrium orbit) is just Δp.

2.2 Matrix Formulation

Taking Δp = 0, at first, we note that both of Eqs. (2.4) are of the form

$$\frac{d^2z}{ds^2} + k(s)\, z = 0 \quad , \tag{2.6}$$

with suitable definition of k(s) and with z being either x or y. From now we work with Eq. (2.6). The function k(s) is periodic with period, C, the circumference of the machine. Perhaps k(s) is periodic in a length $L \leq C$ corresponding to super periods.

We can write the solution of this second order equation as

$$\begin{aligned} (Z(s),\ Z'(s)) &= \begin{pmatrix} M_{11}(s,s_0) & M_{12}(s,s_0) \\ M_{21}(s,s_0) & M_{22}(s,s_0) \end{pmatrix} \begin{pmatrix} Z(s_0) \\ Z'(s_0) \end{pmatrix} , \\ \underline{Z}(s) &= M(s,s_0)\ \underline{Z}\ (s_0) \end{aligned} \tag{2.7}$$

where we have, for convenience used a matrix notation. All of the properties of the machine lattice are in the matrix M which is independent of particular orbits. The determinant of M is proportional to the Wronskian of the two linearly independent solutions obtained by starting with (1) unit amplitude and zero slope and (2) zero amplitude and unit slope. Thus the determinant of M is a constant and equal to unity.

It is clear that if the lattice is made up of sections, then the matrix M for transport through the full lattice is just obtained by successively multiplying the matrices for each section.

If the focusing function k(s) is constant, and piece-wise constants cover just about all cases one meets in practice, then the matrix M is simply

$$M(S,S_0) = \begin{pmatrix} \cos\phi & \frac{1}{\sqrt{k}}\sin\phi \\ -\sqrt{k}\sin\phi & \cos\phi \end{pmatrix}, \qquad (2.8)$$

where $\phi = \sqrt{k}\,(s - s_0)$. This form is convenient if $k > 0$. If $k < 0$ then M simply transforms to:

$$M(s,s_0) = \begin{pmatrix} \cosh\theta & \frac{1}{\sqrt{-k}}\sinh\theta \\ \sqrt{-k}\sinh\theta & \cosh\theta \end{pmatrix}, \qquad (2.9)$$

where $\theta = \sqrt{-k}\,(s - s_0)$. Note that both of these specific forms for M satisfy the requirement $\det M = 1$.

2.3 The α, β, γ Formalism

Any 2 x 2 matrix can be written in the form

$$M = \begin{pmatrix} \cos\mu + \alpha\sin\mu & \beta\sin\mu \\ -\gamma\sin\mu & \cos\mu - \alpha\sin\mu \end{pmatrix}. \qquad (2.10)$$

Since our M has unit determinant

$$\gamma = \frac{1+\alpha^2}{\beta}\ . \qquad (2.11)$$

Notice that M^k can be written in the compact form:

$$M^k = \begin{pmatrix} \cos k\mu + \alpha\sin k\mu & \beta\sin k\mu \\ -\gamma\sin k\mu & \cos k\mu - \alpha\sin k\mu \end{pmatrix}. \qquad (2.12)$$

Thus, for example, if M describes the motion once around the accelerator then M^k describes k-circuits of the machine. It is evident, from Eq. (2.12), that if μ is real then all the elements of M^k are bounded and hence that the motion is stable. A necessary and sufficient condition for stability is simply

$$|\ \text{Trace } M\ | \leq 2\ . \qquad (2.13)$$

It is evident that we can find differential equations that are satisfied by α, β, γ. Why, you ask, should the single equation (Eq. (2.6)) be replaced with equations for α, β, γ? The thought is simple: The original equation was for a particle orbit and hence the initial conditions of special orbits come in. If we get equations for α, β, γ we can get free of particular orbits.

Perhaps the easiest way to proceed is to invoke Floquet's theorem, which states that two independent solutions of Eq. (2.6), with k(s) satisfying a periodic condition with L the period, are

$$z_1(s) = P_1(s)\, e^{+i\frac{\mu s}{L}}\ ,$$

$$z_2(s) = P_2(s)\, e^{-i\frac{\mu s}{L}}\ , \qquad (2.14)$$

where P_1 and P_2 are periodic functions having the same period L. Now one can show that (a problem for the reader!):

$$\frac{d\beta}{ds} = -2\alpha\ ,$$

$$\frac{d\alpha}{ds} = k\beta - \gamma\ , \qquad (2.15)$$

and, of course, Eq. (2.11).

One can now write the solution, Eq. (2.14) in terms of these parameters and obtains (another problem for the reader!)

$$z_{\binom{1}{2}}(s) = C\beta(s)^{1/2}\, e^{\pm i\phi(s)}\ , \qquad (2.16)$$

where C is a constant and the phase advance $\phi(s)$ is given by

$$\phi(s) = \int \frac{ds}{\beta(s)}\ . \qquad (2.17)$$

The form of Eq. (2.16) is often used in describing accelerators. Notice that <u>all</u> the machine focusing parameters are in the function $\beta(s)$. The amplitude is proportional to $\beta^{1/2}$ ("Low β" makes small beams which is good for a colliding beam point) and the local wavelength is $2\pi\beta$. (At a "low-β" point, a focus, the particles have a lot of transverse momenta, go at large angles, which is good for a crossing because then the kick from the other beam is relatively less effective.)

From Eq. (2.16) and Eq. (2.14) we see that if we integrate Eq. (2.17) over one machine circumference then

$$2\pi Q \equiv \mu\Big|_{\substack{\text{one}\\ \text{circumference}}} = \int_0^C \frac{ds}{\beta(s)}\ , \qquad (2.18)$$

where the "Q-value" is simply the number of betatron oscillations per turn. Often Q is called the "tune."

In terms of α, β, γ we can form the quantity

$$\epsilon = \pi\,\frac{z^2 + (\alpha z + \beta z')^2}{\beta}\ , \qquad (2.19)$$

which is an invariant, first introduced by Courant & Snyder. They, with Livingston, invented the very concept of "strong focusing"; i.e. allowing k to be a function of S rather than a constant. Demonstration that the emittance, ϵ, is a constant of the motion is left as still another exercise for the reader.

Typically ϵ will be limited by some aperture stop; i.e. the accelerator has an acceptance which is less than the emittance of the beam (ion source). Matching of acceptance (or admittance) and emittance is a big subject. Clearly, it is relevant to many aspects of beam handling.

Since Eq. (2.19) is simply an ellipse for any values of α, β, γ the focusing properties of a lattice can be completely described by the motion of this ellipse. The relation between the invariant ellipse and the parameters α, β, γ is shown in Fig. 1. Since particles are usually completely distributed in phase the ellipse curve is uniformly occupied. Thus we only need to study how the ellipse rotates, stretches, and distorts (but keeps the same area!) as we move through the lattice.

2.4 The Dispersion Function, Momentum Compaction, & Chromaticity

In the last section we took a particle with $\Delta p = 0$; i.e. having the same energy as that of the reference particle. We now want to consider the effect of a non-zero Δp.

The dispersion, $\eta(s)$, is defined as the periodic solution of the first equation of Eq. (2.4). It isn't difficult to show that

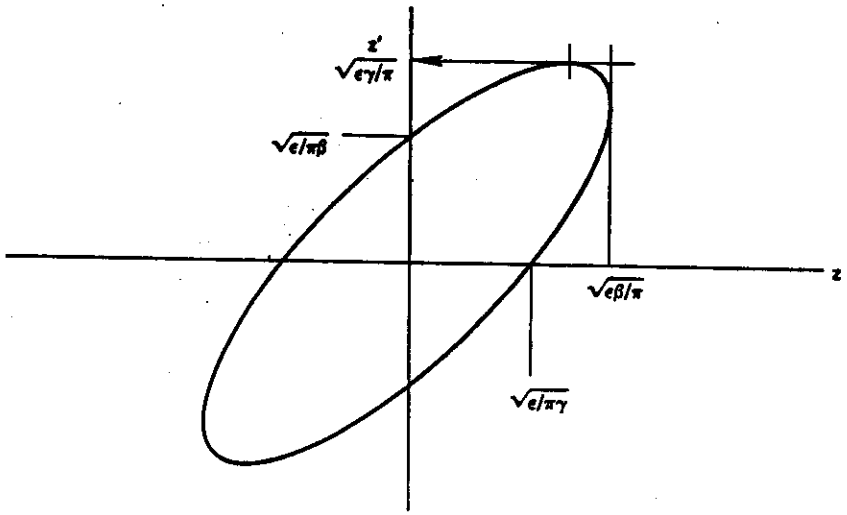

Fig. 1. The invariant ellipse, of area ϵ, and some of its special dimensions in terms of α, β, γ.

$$\eta(s) = \frac{\beta^{1/2}(s)}{2 \sin \pi Q} \int_0^C \frac{\beta^{1/2}(x)}{\rho(x)} \cos\left[\mu(x)-\mu(s)-\pi Q\right] dx \quad , \tag{2.20}$$

The average value, over a circumference, of the dispersion is called the momentum compaction times the radius, $R\alpha$. Since $\bar{\eta} \approx R/Q^2$, $\alpha \approx 1/Q^2$. One can see that the name is very physical for α is a measure of how compacted in transverse space are particles of different momenta.

The chromaticity, ξ, is defined by

$$\xi = \frac{\Delta Q/Q}{\Delta p/p} \; ; \tag{2.21}$$

i.e. by the variation in tune with momenta. We will see that ξ comes into an analysis of the coupling between energy oscillations and transverse oscillations (The Head-Tail Effect).

2.5 Thin Lens Approximation

We can often employ thin lenses, rather than the thick lenses of Eqs. (2.8) and (2.9). This is a good approximation frequently, and even if it isn't adequate for detailed numerical predictions it can be used to give insight.

In the thin lens approximation we simply let the arc length, $s-s_0$, in Eqs. (2.8) and (2.9) go to zero. Thus we get, for a focusing lens

$$M_+ = \begin{pmatrix} 1 & 0 \\ -1/f_+ & 1 \end{pmatrix} \quad , \tag{2.22}$$

where f_+ is simply the focal length of the lens; that is

$$1/f_+ = k\ell \quad . \tag{2.23}$$

Similarly, for a defocusing lens

$$M_- = \begin{pmatrix} 1 & 0 \\ 1/f_- & 1 \end{pmatrix} \quad , \tag{2.24}$$

where

$$1/f_- = |k|\ell, \tag{2.25}$$

and $(-f_-)$ is simply the focal length of the defocusing lens.

2.6 The FODO Lattice

A very good lattice for high energy machines, it has been used in the FNAL main ring and PEP and the SPS, is the FODO lattice which is shown in Fig. 2.

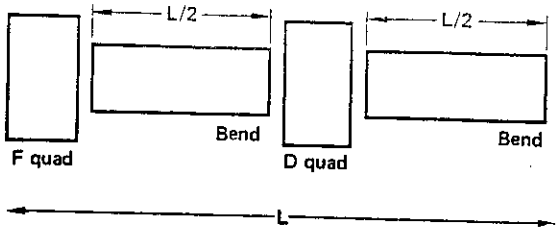

Fig. 2. The FODO Lattice

We can make a thin lens approximation to this lattice and determine all of its properties. Thus, starting at a bend magnet we have:

$$M = \begin{pmatrix} 1 & 0 \\ -1/f & 1 \end{pmatrix} \begin{pmatrix} 1 & L/2 \\ 0 & 1 \end{pmatrix} \begin{pmatrix} 1 & 0 \\ 1/f & 1 \end{pmatrix} \begin{pmatrix} 1 & L/2 \\ 0 & 1 \end{pmatrix} , \qquad (2.26)$$

where we have introduced (the obvious) matrices for the drift through a bend magnet which doesn't focus but simply bends.

The reader might want to carry this through and determine α, β, γ as functions of position, as well as to determine conditions on f and L to give focusing (in both planes!). One finds that

$$\mu = 2 \sin^{-1} \left(\frac{L}{4f} \right) . \qquad (2.27)$$

In addition, the dispersion $\eta(s)$ and then the momentum compaction and chromaticity can be determined.

2.7 Straight Sections and Low-β Insertions

Accelerators need free spaces for injection, rf cavities, extraction, etc. They also need low-β intersection regions. We have developed a formalism which covers these cases, but we haven't explicitly discussed the subject.

Generally, one proceeds by making "insertions"; i.e. sections which don't affect particle motion in the rest of the lattice. Thus one can first optimize the lattice and then design inserts as needed.

A possible long straight section is shown in Fig. 3. This insert has a phase advance of $\pi/2$ and in thin lens approximation

$$s_1 = 1/\gamma ,$$

$$s_2 = \alpha^2 \, 1/\gamma ,$$

$$\frac{1}{f} = \frac{\gamma}{\alpha} , \qquad (2.28)$$

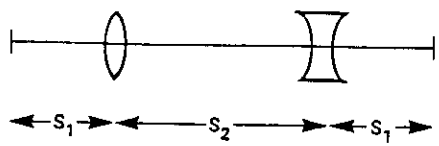

Fig. 3. A Collins Straight section

where α, γ are the parameters of the normal lattice at the "break point" where the straight section is inserted.

Notice that the length of the straight section is (roughly) β. Matching can be achieved in both transverse planes if $\alpha_x = -\alpha_y$, $\gamma_x = \gamma_y$ at the break point. If the dispersion and its derivative (η, η') are both zero at the break point then the insert will not change η (or α).

The design of lattices is an art to which people devote their whole lives. A number of computer programs (Synch, Magic, AGS, Transport) exist to aid in this process for it is exceedingly complicated since many choices are at hand and better choices cost less, accomplish more, or do both simultaneously.

The design of low-β sections is dominated by the variation of β in a free-space region. (We consider a free region for detection of the reaction products; having nearby magnets would help!). From Eq. (2.15) we obtain in a region where $k = 0$

$$\beta \frac{d^2\beta}{ds^2} - \frac{1}{2} \left(\frac{d\beta}{ds} \right)^2 - 2 = 0 . \qquad (2.29)$$

This has solution

$$\beta(s) = \beta(0) + \frac{s^2}{\beta(0)} , \qquad (2.30)$$

where $\beta(0)$ is the value of β at the crossing point. The very first quadrupoles must turn β around and, because β is large there (probably larger than anyplace else in the lattice), the beam is most sensitive to imperfections in the field or displacements of that quadrupole. This sensitivity; i.e. tolerances in the construction of the first quadrupoles, is what puts the limit on how low $\beta(0)$ can be made.

2.8 Machine Imperfections and Coupling Resonances

Up to this point we have been thinking of a perfect machine. No such thing exists and there is, naturally, a highly developed field of random errors, misalignments, etc.

Suppose there is an error in field, ΔB, which extends over a length L. It is easy to show that just at the error position the periodic orbit is displaced from the periodic orbit when $\Delta B = 0$ by

$$u = \frac{1}{2}\,\beta\,\frac{(\Delta B)\,L}{B\rho}\cot \pi Q \quad . \tag{2.31}$$

Thus integral values of Q are bad because the new equilibrium orbit is outside the machine. In designing a machine one must stay away from integral values of Q.

Suppose there is a gradient error; i.e. a thin lens of focal length f is introduced into the lattice. Then, the new tune value is given by

$$\cos \mu = \cos \mu_0 + \frac{\beta_0}{2f} \sin \mu_0 \quad . \tag{2.32}$$

(Remember $Q = \mu/2\pi$.) If we let

$$\mu = \mu_0 + \Delta\mu \quad , \tag{2.33}$$

then for $\Delta\mu \ll \mu_0$ we have, provided $\sin \mu_0 \neq 0$,

$$\Delta\mu = -\frac{\beta_0}{2f} \tag{2.34}$$

$$\text{or } \Delta Q = -\frac{\beta_0}{4\pi f} \quad . \tag{2.35}$$

Thus there is a tune shift provided Q_0 is not an integer or a half-integer. If Q_0 is half-integral or integral that is bad for the motion becomes unstable. One must design machines to avoid these values. How wide is the stop band? Clearly

$$\delta Q = \frac{\beta_0}{2\pi f}, \tag{2.36}$$

and this small band must be avoided.

In an ideal machine the two transverse planes are independent. Field errors introduce coupling and the Eqs. (2.4) become:

$$\begin{aligned} \frac{d^2x}{ds^2} + k_x\, x &= \frac{y}{B\rho}\,\frac{\partial B_y}{\partial y} - \frac{B_s}{B\rho}\,\frac{dy}{ds} \quad , \\ \frac{d^2y}{ds^2} + k_y\, y &= -\frac{x}{B\rho}\,\frac{\partial B_x}{\partial x} + \frac{B_s}{B\rho}\,\frac{dx}{ds} \quad , \end{aligned} \tag{2.37}$$

where B_s is the field along an orbit. (For example a solenoid.)

The analysis of coupling shows that this can be large when

$$\begin{aligned} Q_x + Q_y &= \text{integer} \quad , \\ Q_x - Q_y &= \text{integer} \quad . \end{aligned} \tag{2.38}$$

These values, also, must be avoided; especially the "sum resonance" (the + sign) where both x and y motion becomes unstable and grows exponentially.

Non-linearities add to this subject, but we can't go into that in this article.

III. TRANSVERSE MOTION: NONLINEARITIES

Is the solar system stable? Clearly it is for short times ($\approx 10^{10}$ years), but what about for long times? It consists of 10 major bodies, and thousands of minor bodies. What is the eventual configuration? Will, for example, one of the larger bodies fall into the sun and the other planets escape to infinity (while overall energy is conserved)?

The planets move near equilibrium orbits which are, approximately, ellipses. The small deviations from these orbits can be shown to be linearly stable. What, however, will the effect be of the non-linearities?

Thus one can see that the situation is very similar to that in a particle accelerator which has been designed, according to the theory of Section II, so as to be linearly stable. In this section we address the effect of non-linearities on the linearly stable motion of particles. The first part is devoted to a general discussion and the second to a particular, but terribly important, aspect of non-linear phenomena.

3.1 The KAM Theorem

Starting in the 1960s there has been a revolution in classical mechanics. Whole conferences are now devoted to stochasticity, solitons, strange attractors, and the routes to turbulence. Much of this work is built upon that of Kolmogorov, while the mathematicians Arnold and Moser, who rigorously proved the (correct) intuitive approach of Kolmogorov, where both, even at the time, very aware -- even motivated by -- the importance of this work to accelerators.

The KAM Theorem, which takes hundreds of pages to prove, and many pages to state precisely, is (roughly) the following: Consider a system of N degrees of freedom governed by the Hamiltonian

$$H = (1/2)\sum_{k=1}^{N}\left(P_k^2 + \omega_k^2\, Q_k^2\right) + \lambda\,[V_3 + V_4 + \ldots] \quad , \tag{3.1}$$

where ω_k are real frequencies, V_3 and V_4 are cubic and quartic polynomials in P_k and Q_k, and λ is a measure of the nonlinearities. Suppose that:

1) $\sum_k n_k\,\omega_k \neq 0$; for any integers n_k such that $\sum_k |n_k| \leq 4$

(That is; that low-order linear resonances are avoided.),

2) λ is sufficiently small (but not infinitesimal, so the non-linearities are small),

3) V_3 is non-zero. (So there is some cubic non-linearity.)

Then, the theorem states that except for a set of small measure, the trajectories are quasi-periodic orbits lying on a smooth N-dimensional surface in the 2 N-dimensional phase space.

Thus it has been proved that some non-linear (i.e. "real") dynamical systems are not ergodic. In particular, a one-dimensional non-linear system has a non-zero stable region around a linear stable equilibrium point, with the phase plane looking like that in Fig. 4. For an N-dimensional system -- there may be instability due to "resonance streaming," "Arnold diffusion," or by "modulational diffusion." Generally, for small non-linearities these processes are negligibly small.

For large non-linearity the system is wildly unstable; i.e. trajectories which are initially close to each other separate at an exponential rate. The system is said to be stochastic.

The dividing line between these two situations is a much-studied subject. It is given (roughly) by the Chirikov condition which is just that the separation between stable regions (buckets) be equal to the extent of the stable region (height of the bucket). (Clearly one only takes the nearest resonance into account when computing the extent of the stable region.)

3.2 Beam-Beam Interaction

The interaction of one beam with another is, generally, a many-body problem, but we can consider (and still get most of the physics) the interaction of a single particle with a charge and current distribution ("weak-strong" beams). If we restrict ourselves to this case we are simply studying a non-linear dynamics problem and it has many of the features outlined above.

Consider, for simplicity, the head-on collision of one particle with a bunch of N_b particles. Suppose the bunch has length ℓ, width w, and height h. If w >> h we need only consider the vertical force which is linearly varying inside the bunch and then drops-off for larger vertical distance y. The electric field inside the beam is

$$E_y = \left(\frac{4\pi N_b e}{\ell w h}\right) y \quad . \tag{3.2}$$

This electric field will change the particles momentum by

$$\Delta p_y = (eE)\left(\frac{\ell}{2c}\right)(2) \quad , \tag{3.3}$$

where the time factor comes from the fact that the particle and the bunch are both moving at the velocity c, and the factor of 2 comes because the magnetic force is just equal to the electric force.

$$\Delta\left(\frac{dy}{ds}\right) \equiv \Delta y' = \frac{\Delta p_y}{p} = \frac{4\pi N_b e^2 \ell y}{\ell w h c m c \gamma} \quad . \tag{3.4}$$

Fig. 4. The phase plane of one dimensional motion around a stable fixed point. Notice the regions of instability (x-points) alternating with regions of stability.

The change in tune, ΔQ, is just

$$\Delta Q = \left(\frac{\beta}{4\pi}\right)\left(\frac{\Delta y'}{y}\right) , \qquad (3.5)$$

in terms of the β-function at the crossing point. Combining Eq. (3.5) and (3.4) we have

$$\Delta Q = \frac{N_b\, r_0 \beta}{w\, h\, \gamma} , \qquad (3.6)$$

where we have introduced the classical particle radius $r_0 = e^2/mc^2$.

Now, if the kick were really linear then as long as ΔQ is not large enough to shift one to a machine resonance there is no problem. But experimentally it is observed that even with $\Delta Q = 0.02$ (a very small number!) there is wild blow-up of the beam. Thus the "linear tune shift," Eq. (3.6), is a measure of non-linear phenomena. Consequences of Eq. (3.6), and the development of "low-β" sections (clearly a good direction) will be covered in the lectures on specific machines.

Theoretical study of the beam-beam phenomena is a very large subject. (Whole conferences have been devoted to it.) Suffice it to say that many dimensional (3) particle simulations are in good accord with the observations and with the basic physics that is described in Sec. 3.1.

IV. LONGITUDINAL MOTION

The longitudinal motion of particles in an accelerator received special attention with the discovery of phase stability by McMillan and Veksler. Subsequently, the special problems associated with storage rings caused a re-examination and new formulation of the theoretical framework of the subject.

4.1 Basic Equations

A particle, of energy γmc^2, circulating in a particle accelerator will have an orbital frequency f. A particle of slightly different energy will have a slightly different frequency and the relation between these two quantities is the dispersion in revolution frequency, η, defined by

$$\frac{df}{dp} = -\frac{f}{p}\eta . \qquad (4.1)$$

The dispersion η has two contributions: A particle of energy slightly larger than that of the reference particle, will slip out to an equilibrium orbit of greater length (and hence have its frequency reduced), but move at a greater speed (and hence have its frequency increased). These two effects fight each other with the first clearly winning at high energies where a particle hardly can increase its speed. A typical figure is as shown in Fig. 5. We can show that

$$\eta = \alpha - \frac{1}{\gamma^2} \equiv \frac{1}{\gamma_t^2} - \frac{1}{\gamma^2} , \qquad (4.2)$$

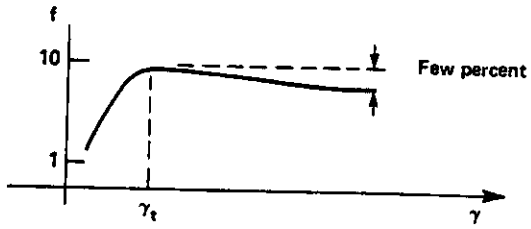

Fig. 5. Frequency vs energy in a typical accelerator.

where α is the momentum compaction factor and the transition energy, γ_t, is defined by $\gamma_t^2 = 1/\alpha$.

Consider an accelerator with only one accelerating cavity which is localized in azimuth and has an rf voltage impressed upon it so that the voltage across the cavity is

$$V = V_0 \sin 2\pi f_{rf} t , \qquad (4.3)$$

where the amplitude V_0 and the frequency f_{rf} could be (slowly) changing in time.

Let ϕ be the phase of a particle relative to the rf. Clearly, on passing the cavity the particle will have its energy augmented so that

$$\frac{dE}{dt} = eV_0 f \sin\phi , \qquad (4.4)$$

where f is the particle revolution frequency. The phase, ϕ, changes if f is not equal to f_{rf}. Thus

$$\frac{d\phi}{dt} = 2\pi (f_{rf} - hf) , \qquad (4.5)$$

where the integer h is the harmonic number of the rf.

These two equations, Eqs. (4.4) and (4.5), are the basic equations describing the energy oscillations, or longitudinal motion, of a particle. Combining them, by taking the derivative of Eq. (4.5):

$$\frac{d^2\phi}{dt^2} = 2\pi\left(\frac{df_{rf}}{dt} - h\frac{df}{dE}\frac{dE}{dt}\right) . \qquad (4.6)$$

Using Eq. (4.4):

$$\frac{d^2\phi}{dt^2} = 2\pi\frac{df_{rf}}{dt} - 2\pi h\frac{df}{dE} eV_0 f \sin\phi . \qquad (4.7)$$

If the rf frequency is not modulated, and using the definition of Eq. (4.1),

$$\frac{d^2\phi}{dt^2} - (2\pi)\frac{hf^2}{E}\eta eV_0 \sin\phi = 0 \quad . \tag{4.8}$$

Thus for ϕ near zero there are small stable oscillations at the synchrotron frequency:

$$\omega_s^2 = (2\pi f)^2 \frac{heV_0(-\eta)}{2\pi E} \quad , \tag{4.9}$$

provided $(-\eta)$ is positive. At transition the sign of η changes and, hence, the phase of the rf must be quickly changed by 90° so as to keep the particle motion stable.

The motion is described by Eq. (4.8), which is an integrable system, so that one can easily study non-linear phenomena. These phenomena are very important in the design of systems which efficiently trap particles at injection, or in systems which properly "stack" particles; i.e. make the intense hadron beams one needs for collisions. A Hamiltonian formalism is most advantageous for these studies since the motion is rather complicated and the use of general theorems, such as Liouville's, proves very powerful.

4.2 Hamiltonian Formalism

Introduce the "energy" variable w, which is like an angular momentum, by

$$w = \frac{E}{2\pi f} \quad . \tag{4.10}$$

Then the Hamiltonian

$$H(\phi,w) = \left(\frac{h\eta 2\pi f}{2pR}\right) w^2 + \frac{eV_0}{2\pi}\left[\cos\phi - \cos\phi_0 + (\phi-\phi_0)\sin\phi_0\right] \quad , \tag{4.11}$$

where ϕ_0 is the phase of the reference particle, gives the equations of motion

$$\frac{d\phi}{dt} = \frac{\partial H}{\partial w} = \frac{h\eta(2\pi f)}{pR} w \quad ,$$

$$\frac{dw}{dt} = -\frac{\partial H}{\partial \phi} = \frac{eV_0}{2\pi}\left[\sin\phi - \sin\phi_0\right] \quad , \tag{4.12}$$

which are just our basic equations in a slightly different notation.

Using this Hamiltonian we can, easily, study the size of the stable region of oscillation (the "bucket"), non-linear variation of the synchrotron frequency, criteria for adiabatic variation of V_0 and ϕ_0, etc.

V. ADIABATIC VARIATION

Accelerators are designed, after all, to accelerate particles. So far, our discussion has been restricted to parameters which are constant in time and we now must generalize our work. The point is, of course, that the synchrotron oscillation frequency, the circulation frequency, and the betatron frequencies are all larger than the frequencies with which parameters change. (This doesn't have to be so for rf modulation and synchrotron frequencies, but one tries to observe the inequality in practice.)

Thus acceleration, and injection and rf stacking, etc. are all adiabatic processes. Thus all of our previous analysis is valid; i.e. it describes properly the oscillations of particles. Any conditions we derived, and we really determined many conditions on the lattice elements and rf system, must all be observed.

What happens as we change parameters slowly; i.e. adiabaticly? If we formulate the theory in a Hamiltonian formalism then the answer is very simple for the theory of adiabatic invariants, or the change of diverse variables under change of parameters, is well worked out.

Take, for example, the longitudinal motion. The canonical variables are ϕ and w and hence

$$\int w\, d\phi = \text{constant} \quad . \tag{5.1}$$

Thus if we take particles from one energy E, to a second energy E_2, and in both cases they occupy all phases then the spread at energy E_2, ΔE_2, is related to the spread at energy E_1, ΔE_1 by

$$\Delta E_2 = \Delta E_1 \left(\frac{f_2}{f_1}\right) \quad . \tag{5.2}$$

A very significant question in building-up intense hadron beams for collision is how best to do this. The Hamiltonian formulation gives insight into this process which has, quite naturally, been studied very extensively.

For transverse motion it is easy to show that the emittance, ε, decreases as $\beta\gamma$. (Here β and γ are the relativistic factors not the orbit parameters α, β, γ.) Thus the transverse size of beams damps and beams get smaller as the energy is increased. Thus one has millimeter size beams at Fermilab as contrasted with the many centimeter size beams at the Bevatron. (Note that the minor radius only damps (for $\beta \approx 1$) as the square root of the energy.)

PART B: COLLECTIVE EFFECTS

VI. EQUILIBRIUM LIMITS

The performance of accelerators is, in general, determined by collective phenomena. (The beam-beam phenomena, considered in Sec. III, which is often a limit on performance but is, of course, a collective effect.)

Block diagram of the Single Particle Motion approach
to self-field phenomena

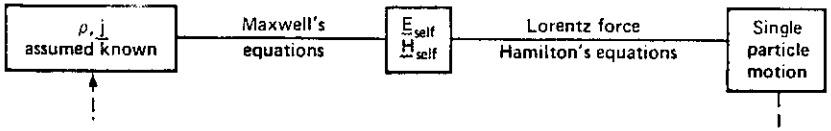

Fig. .6 Block diagram of the single-particle approach self-field phenomena.

Analysis proceeds by considering, firstly, equilibrium limits and then, secondly, possible instabilities of the equilibrium. This was, in fact, the historical path for it wasn't until the 1950s that it was realized that instabilities of relativistic particle beams were possible and, furthermore, imposed severe limits on accelerator performance.

Simple-mindedly, one can proceed as shown in Fig. 6. This approach can always be used, but most of the literature employs the approach shown in Fig. 7; i.e. using the collisionless Boltzmann equation or the Vlasov equation. We shall, in this section, follow the approach of Fig. 6; in the next section we shall follow the method Fig. 7.

Firstly, however, we must find the equilibrium configuration, and as we shall quickly see, there is a space charge limit. In fact, this was realized first, in 1940, by Kerst and Serber. Subsequently, of course, this calculation has been done for much more general geometry.

A very simple approach assumes that we have N particles in a cylindrical beam of minor radius, a, going in a circle of radius, R. For R >> a, we can ignore the curvature and taking a coordinate system as indicated in Fig. 8, we have;

$$\rho = \begin{cases} \dfrac{Ne}{(2\pi R)(\pi a^2)} & ; \quad r \leq a \\ 0 & ; \quad r > a \end{cases} \qquad (6.1)$$

$$\underset{\sim}{j} = \rho \beta c \, \hat{\underset{\sim}{j}} \ ,$$

where $(\rho, \underset{\sim}{j})$ are the beam charge density and current density.

From Maxwell's equations, the self electric and magnetic fields are:

$$\underset{\sim}{E}_{self} = 2\pi\rho(z \, \hat{\underset{\sim}{k}} + x \, \hat{\underset{\sim}{i}}) \ ,$$

$$\underset{\sim}{H}_{self} = 2\pi\rho\beta(z \, \hat{\underset{\sim}{i}} - x \, \hat{\underset{\sim}{k}}) \ , \qquad (6.2)$$

for r less than a.

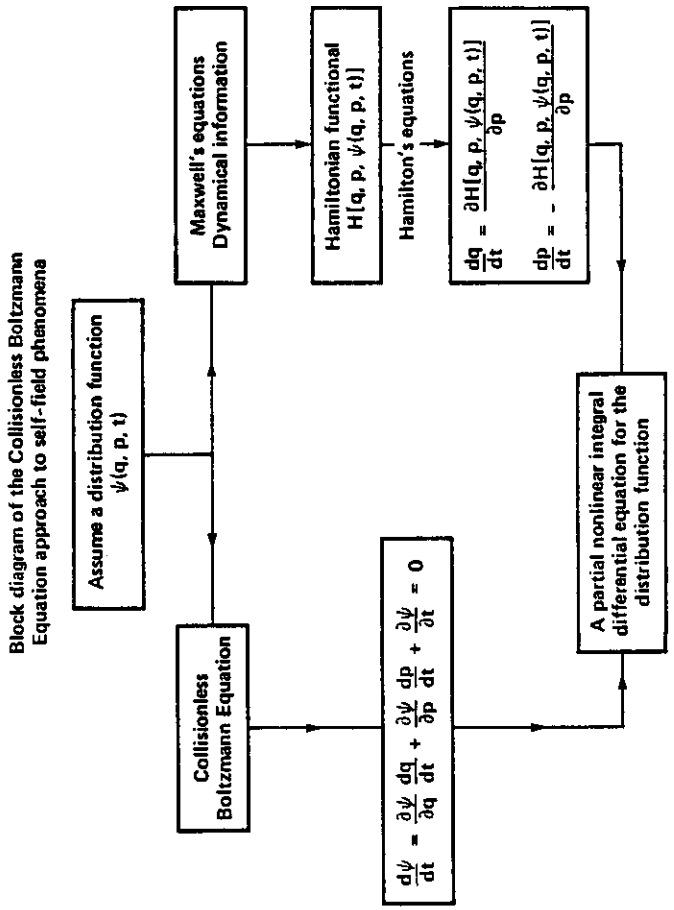

Fig. 7. Block diagram of the collisionless Boltzmann equation approach to self-field phenomena.

The Lorentz force and Hamilton's equations, note how we are just following the procedure of Fig. 6, imply

$$\gamma m \frac{d^2 x}{dt^2} = e\,(E_x - \beta H_x) \quad , \tag{6.3}$$

or using Eq. (5.2) and remembering that there is an external guide field:

$$\gamma m \frac{d^2 x}{dt^2} = 2\pi \rho e\,(1 - \beta^2) x - e\beta \frac{\partial B_0}{\partial z}\, x \quad . \tag{6.4}$$

Letting

$$Q_0^{\,2} = \frac{R}{B_0} \frac{\partial B_0}{\partial z} \quad , \tag{6.5}$$

and introducing the classical electron (proton) radius

$$r_0 = \frac{e^2}{mc^2} \quad , \tag{6.6}$$

the solution is

$$x \sim e^{iQ\theta} \quad , \tag{6.7}$$

where we have now bent the coordinate system so that $z \to R\theta$. Clearly,

$$Q^2 - Q_0^{\,2} = - \frac{2\pi R^2 e \rho}{\gamma^3 m \beta^2 c^2} \quad , \tag{6.8}$$

or, using Eq. (6.1),

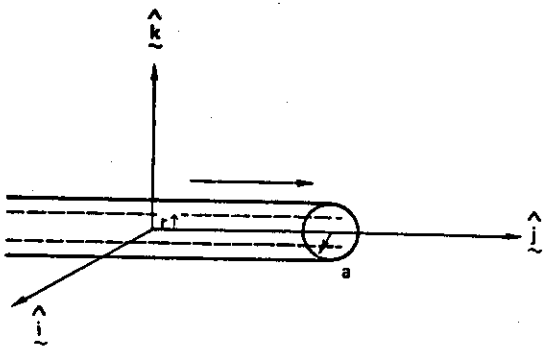

Fig. 8. Coordinate system for a simple derivation of the transverse space charge limit. The beam moves in direction j.

$$N = - \frac{\pi a^2 \gamma^3 \beta^2}{R^2 r_0} (\Delta Q^2) \quad . \tag{6.9}$$

Now we know from our work on machine resonances, Sec. 2.8, that there is a limit on ΔQ^2 in order not to displace the operating point, Q_0, to the nearest resonance; roughly that $\Delta Q \approx 1/4$. Thus we have found an equilibrium space charge limit. Our work needs to be, and has been, extended to elliptical beams and, also, curvature has been included. Most importantly, image effects have been included by Laslett, and these reduce the γ^3 to γ. (The reason is that the precise cancellation, seen in Eq. (6.4), is no longer true.) Of course this is a most significant modification at high energies although it is nevertheless generally true that the equilibrium space charge limit is not the limit in high energy accelerators -- other limits come in first.

VII. LONGITUDINAL INSTABILITY

The simplest collective effect is longitudinal in a beam which in equilibrium is uniform in azimuth. This is because, to good approximation, one has only one degree of freedom; namely the longitudinal coordinate or azimuthal angle. Much can be learned from studying this problem: all of the basic physics, really, and an approach which can be used in much more complicated situations. In fact, it was this instability which was first analyzed, and purely theoretically at that. Subsequently, the effect was found experimentally and still, to this day, imposes a severe limit on machine performance.

7.1 The Negative Mass Effect

In the first half of the nineteenth century the composition of Saturn's rings was a subject of considerable interest. Although one possibility was that a ring consists of many small rocks, this was considered unlikely for such a configuration is staticly unstable (since under mutual gravitational attraction the rocks will coalesce into one moon). Thus in 1856 the Adam's Prize was to be given to the most illuminating essay on subject of Saturn's rings.

The prize was won by a 25-year-old who was, however, not unknown. For 10 years previously he had his first paper read at the Royal Society of Edinborough. Subsequently, James Clerk Maxwell was to make many important contributions to physics, but his prize-winning essay was characterized by the great mathematician, Sir George Airy, as "one of the most remarkable applications of Mathematics to Physics that has ever been seen."

Maxwell's argument was, essentially, the following. Let M be the mass of Saturn and m be the mass of one rock moving with velocity v in a ring of radius R. Balancing gravitational attraction with centripetal force:

$$\frac{GMm}{R^2} = \frac{mv^2}{R} \quad . \tag{7.1}$$

The frequency, f, of the rock is:

$$f = \frac{v}{2\pi R} = \frac{1}{2\pi R} \sqrt{\frac{GM}{R}} \quad , \tag{7.2}$$

The energy, E, of the rock is:

$$E = (1/2)\, mv^2 - \frac{GMm}{R} = -(1/2)\, \frac{GMm}{R} \quad . \tag{7.3}$$

Combining these last two equations:

$$f = \frac{(-E)}{\pi GMm} \sqrt{\frac{2(-E)}{m}} \quad . \tag{7.4}$$

The variation of these last equations is shown in Fig. 9.

The many-body argument goes the following way. (Up to now the analysis, has been trivial. Now, suddenly, we are going to consider a many-body situation. The analysis jumps in complexity by orders of magnitude; yet it is all done in two sentences. Think deeply!) Consider a region of the ring where, for some reason (a fluctuation), the density is higher than the average. A rock in front of this increase will be pulled back and so its energy decreases and, hence, its frequency increases and so it moves ahead. (Clearly, an analagous argument can be made for a rock behind.) Hence a ring which is staticly unstable is dynamically stable.

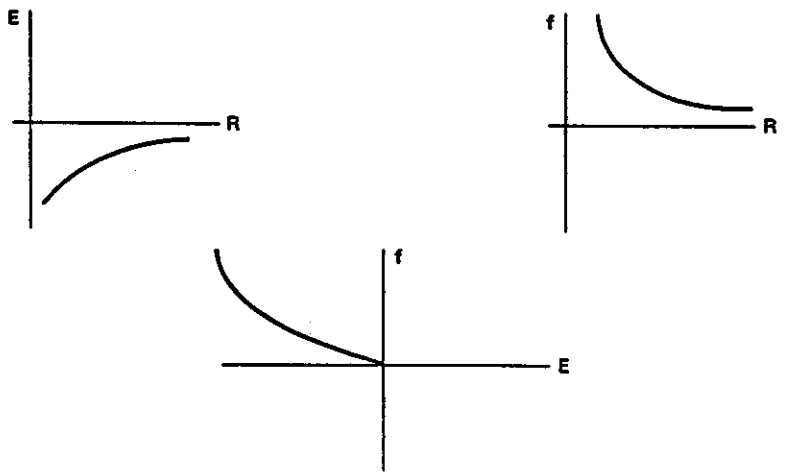

Fig. 9. Variations of f, E, and R for a satellite. It is well-known, in this space age, that as E decreases f increases; i.e. that satellites "go faster" (angularly) as they slow down.

Now it is clear that in a particle beam we have repulsion, not attraction, and thus a staticly stable situation is dynamically unstable. (Historically, this dynamical instability was discovered by accelerator physicists and it was only subsequently that they appreciated that Maxwell had been there 100 years earlier.) It is as if the particles have a "negative mass"; i.e. repulsive forces produce attraction.

We shall now give an analysis of the negative mass effect using the approach of Fig. 7. Thus we describe the particles by a distribution function $\psi(\phi, \dot{\phi}, t)$, where ϕ is the azimuthal angle. The distribution function ψ satisfies to very good approximation the collisionless Boltzmann equation. (I realize we are not working in terms of canonical coordinates and momenta, but Liouville's theorem is valid in this ϕ-$\dot{\phi}$ space.) (By ignoring collisions we are neglecting effects which can, in fact, be treated separate. Some discussion of these effects is given in Sec. IX.

We thus have:

$$\frac{d\psi}{dt} \equiv \frac{\partial \psi}{\partial t} + \dot{\phi}\, \frac{\partial \psi}{\partial \phi} + \frac{d\dot{\phi}}{dt}\, \frac{\partial \psi}{\partial \dot{\phi}} \quad . \tag{7.5}$$

A stationary solution to this equation is given by the arbitrary function $\psi_0(\dot{\phi})$ since there are no forces which tend to change ϕ in time. In a "coasting beam" we can arbitrarily choose the distribution of particles over energy, which is, of course, the same statement.

Let us look for small variations from this solution by letting

$$\psi(\phi, \dot{\phi}, t) = \psi_0(\dot{\phi}) + \psi_1(\phi, \dot{\phi}, t) \quad . \tag{7.6}$$

Inserting this into Eq. (7.5) and linearizing the resulting equation we obtain

$$\frac{\partial \psi_1}{\partial t} = -\dot{\phi}\, \frac{\partial \psi_1}{\partial \phi} - \left.\frac{d\dot{\phi}}{dt}\right|_1 \frac{\partial \phi_0}{\partial \dot{\phi}} \quad , \tag{7.7}$$

where $d\dot{\phi}/dt$, which characterizes the force of space charge is linear in ψ_1. Note that ψ_0 does not contribute to $d\dot{\phi}/dt$ since there are no longitudinal forces from a uniform charge distribution.

We need now to evaluate $d\dot{\phi}/dt$ after which Eq. (7.7) is an integral-differential equation for ψ_1. Clearly,

$$\frac{d\dot{\phi}}{dt} = 2\pi \frac{\partial f}{\partial t} \quad , \tag{7.8}$$

where f is the particle frequency.

We may write

$$\frac{\partial f}{\partial t} = \frac{df}{dE}\, \frac{\partial E}{\partial t} \quad , \tag{7.9}$$

and

$$\frac{dE}{dt} = 2\pi R\, f\, e\, E \quad , \tag{7.10}$$

where R is the radius of the orbit, and E is the electric field due to space charge and taken positive in the direction of particle motion. Thus, from Eq. (7.7), we obtain

$$\frac{\partial \psi_1}{\partial t} = -\dot{\phi}\,\frac{\partial \psi_1}{\partial \phi} - 4\pi^2 R\,\left(f\,\frac{df}{dE}\right)_e\, eE\,\frac{\partial \psi_0}{\partial \dot{\phi}} \quad , \tag{7.11}$$

where $(f\, df/dE)_e$ is evaluated for a typical particle in the equilibrium (stationary) distribution $\psi_0(\dot{\phi})$.

The electric field E may be evaluated very easily in the case that the wavelength of the perturbation is large compared to the gap G of the accelerator tank. In this case the electric field may be taken to depend only upon the gradient of the charge distribution at the azimuth in question. Thus

$$E = -\frac{eg}{\gamma^2 R^2}\,\frac{\partial}{\partial \phi}\int \psi_1\,(\phi,\ \dot{\phi},\ t)\, d\dot{\phi} \quad , \tag{7.12}$$

where g is a geometrical factor which depends logarithmicly on the ratio of the gap G, to the radius $\underline{a}$ of the coasting beam, and is given by

$$g = 1 + 2\,\log_e \frac{2G}{\pi a} \quad . \tag{7.13}$$

Inserting this into Eq. (7.11) we obtain:

$$\frac{\partial \psi_1}{\partial t} = -\dot{\phi}\,\frac{\partial \psi_1}{\partial \phi} + \frac{4\pi^2 e^2 g}{\gamma^2 R}\,\left(f\,\frac{df}{dE}\right)_e\,\frac{\partial \psi_0}{\partial \dot{\phi}}\,\frac{\partial}{\partial \phi}\int \psi_1\, d\dot{\phi} \quad , \tag{7.14}$$

which is an linear integral-partial differential equation for ψ_1.

We now seek solutions to Eq. (7.14) of the form

$$\psi_1(\phi,\ \dot{\phi},\ t) = \bar{\psi}_1\,(\dot{\phi})\, e^{\,i\,(n\phi\, -\, \omega t)} \quad , \tag{7.15}$$

where since Eq. (7.14) is linear with real coefficients we may use a complex solution, meaning always either the real or imaginary part. Clearly if ω is imaginary then the mode either grows or decays in time. Inserting Eq. (7.15) into Eq. (7.14) we obtain

$$\bar{\psi}_1(\dot{\phi})(n\dot{\phi} - \omega) = +\frac{4\pi^2 e^2 g}{\gamma^2 R}\,\left(f\,\frac{df}{dE}\right)_e\,\frac{\partial \psi_0}{\partial \dot{\phi}}\, n\int \bar{\psi}_1(\dot{\phi})\, d\dot{\phi} \quad . \tag{7.16}$$

This integral equation for $\bar{\psi}_1(\dot{\phi})$ may be solved immediately since the dependence of $\bar{\psi}_1(\dot{\phi})$ on ϕ is explicit. Let

$$\bar{\psi}_1(\dot{\phi}) = \frac{C\,\dfrac{\partial \psi_0(\dot{\phi})}{\partial \dot{\phi}}}{n\dot{\phi} - \omega} \quad , \tag{7.17}$$

where C is a constant, and insert this into Eq. (7.16) which yields a self-consistency requirement after cancelling C from both sides of the equation, namely:

$$1 = +\frac{4\pi^2 e^2 g}{\gamma^2 R}\,\left(f\,\frac{df}{dE}\right)_e\, n\int \frac{\dfrac{\partial \psi_0(\dot{\phi})}{\partial \dot{\phi}}\, d\dot{\phi}}{n\dot{\phi} - \omega} \quad . \tag{7.18}$$

This equation is a dispersion relation between the "wavelength" n and the "frequency" ω.

For a nearly monoenergetic coasting beam we may take

$$\psi_0(\dot{\phi}) = \begin{cases} \dfrac{N}{2\pi(2\Delta)} & \dot{\phi}_A - \Delta < \dot{\phi} < \dot{\phi}_A + \Delta \\ 0 & \text{otherwise} \end{cases} \quad , \tag{7.19}$$

corresponding to a beam of N particles uniformly spread in "energy" over an interval of width 2Δ, about a mean value $\dot{\phi}_A$. In this case we may readily perform the integral in Eq. (7.18) since

$$\frac{\partial \psi_0(\dot{\phi})}{\partial \dot{\phi}} = \frac{N}{4\pi\Delta}\left\{-\delta\,(\dot{\phi} - \dot{\phi}_A - \Delta) + \delta\,(\dot{\phi} - \dot{\phi}_A + \Delta)\right\} \quad . \tag{7.20}$$

Equation (7.18) becomes

$$1 = \frac{4\pi^2 e^2 g}{\gamma^2 R}\,\left(f\,\frac{df}{dt}\right)_e\, n\,\frac{N}{4\pi\Delta}\left\{\frac{-1}{n(\dot{\phi}_A + \Delta) - \omega} + \frac{1}{n(\dot{\phi}_A - \Delta) - \omega}\right\} , \tag{7.21}$$

or simply, by solving for ω:

$$\omega = n\left\{\dot{\phi}_A \pm \left[\frac{2\pi e^2 gN}{\gamma^2 R}\,\left(f\,\frac{df}{dE}\right)_e + \Delta^2\right]^{1/2}\right\} \quad . \tag{7.22}$$

Thus the perturbation moves with the average speed of the beam, $\dot{\phi}_A$. If Δ is small then for real n, ω will be imaginary for $df/dE < 0$, i.e. for operation above the transition energy. It should be noted that increasing the spread in beam energy (increasing Δ) is always a stabilizing influence. Recalling that the energy spread in the beam ΔE is related to Δ by

$$\Delta E = \frac{2\Delta}{2\pi\left(\dfrac{df}{dE}\right)_e} \quad , \tag{7.23}$$

we may write Eq. (7.22) in the more convenient form:

$$\omega = n \left\{ \dot{\phi}_A \pm \left[\frac{2\pi e^2 gN}{\gamma^2 R} \left(f \frac{df}{dE} \right)_e + \pi^2 \left(\frac{df}{dE} \right)_e^2 (\Delta E)^2 \right]^{1/2} \right\} . \qquad (7.24)$$

Thus if the initial disturbance has n waves about the accelerator, the perturbation will grow as $e^{t/T}$ where the time to increase by a factor of e, T is given by:

$$T = \frac{1}{n} \left\{ + \frac{2\pi e^2 gN}{\gamma^2 R} \left(f \left| \frac{df}{dE} \right| \right)_e - \pi^2 \left(\frac{df}{dE} \right)_e^2 (\Delta E)^2 \right\}^{-1/2} , \qquad (7.25)$$

assuming that $\partial f/\partial E < 0$, and the bracket is positive. If the bracket is negative the motion, of course, is stable. Clearly this expression could be used to find a criterion for stability in any given accelerator.

7.2 Longitudinal Resistive Instability

The negative mass instability, as its very name implies, and consistent with Eq. (7.25) only occurs above the transition energy where $(\partial f/\partial E) < 0$. There, of course, the Landau damping, namely the energy spread within the beam, may be adequately large to prevent instability.

All of this is true on an ideal machine; that is a purely "reactive," in fact capacitive, environment where the electric field E is related to the spacial variation (azimuthally) of the charge density by Eq. (7.12). But this isn't the case in general: Resistive elements will produce a phase shift between E and the derivative of the charge density.

This space shift will produce an instability even below transition! The phase shift is usually quite small, but will have a dramatic effect; a fact that wasn't appreciated until a number of years after the work on the negative mass effect. A great deal of work has now been on this subject and, roughly, one can write that

$$\frac{Z_{\parallel}}{n} \leq \frac{m_0 c^2 |\eta| [\Delta(\beta\gamma)]^2}{e I_0 \gamma} , \qquad (7.26)$$

where I_0 is the beam current and η is the dispersion in revolution frequency; i.e.

$$\frac{\Delta f}{f} = - \eta \frac{\Delta p}{p} , \qquad (7.27)$$

and $Z_{\parallel}$ is the longitudinal coupling impedance of the ring. Note that this relation, which is the analog of the criterion of Eq. (7.25) is only dependent upon $|\eta|$ and must be observed below, as well as above, the transition energy.

7.3 The Coupling Impedance

It was an important step in the understanding of instabilities to realize that the analysis of Sec. 7.1 could be generalized so that one would obtain a relation such as Eq. (7.26) with a coupling impedance $Z_{\parallel}$. Thus the problem shifted to calculating and measuring $Z_{\parallel}$. In fact, in the construction of all modern machines careful track is kept of $Z_{\parallel}$ and of each element's (such as pickup electrodes, kickers, clearing electrodes, rf cavities, etc.) contribution to $Z_{\parallel}$.

For a smooth wall, such as we assumed in Sec. 7.1,

$$Z_{\parallel} = \frac{n Z_0 g}{2\beta\gamma^2} , \qquad (7.28)$$

where Z_0 is the impedance of free space (377 Ω or $4\pi/c$ in Gaussian units).

For other structures, such as those mentioned above, $Z_{\parallel}$ has been calculated. Suffice it to say that if one is very careful then $Z_{\parallel}$ can be kept to 1 to 3 Ω.

VIII. TRANSVERSE INSTABILITY

A transverse instability of a beam; i.e. a coherent, collective, instability, is due to the reaction of the electromagnetic fields caused by an oscillating beam on the particle motion. In this regard it is just like the longitudinal instabilities considered in the last section. The situation is, however, more complicated now since both diverse amplitudes of transverse oscillation and diverse particle momenta will contribute to the Landau damping of the collective oscillation.

Clearly consideration of a uniform beam (a "rubber band") is simpler than consideration of a bunched beam. In the longitudinal case we didn't even treat in these lectures the case of bunched beams! In the transverse case, however, there are many different phenomena associated with bunches than are disclosed by the analysis of uniform beams. One of these phenomena, namely the head-tail effect, is discussed in Sec. 8.2.

8.1 Transverse Resistive Instability

Suppose an azimuthally uniform beam is displaced transversely, or kicked. It will start to oscillate, as we discussed in Sec. II, and will, as a result, excite electromagnetic fields. These fields should be calculated taking into account the surroundings of the beam.

The electromagnetic fields act back on the particle motion. If the fields are precisely in phase then they will simply change the frequency of the oscillation and provided this shift is not great enough to move one to a machine resonance there will be no bad effect. (The reader should contrast this with the longitudinal case where the negative mass made the situation very different indeed.)

If, however, there is an out-of-phase component due, perhaps, to the finite resistivity of the wall then the original oscillations can be reinforced; i.e. there can be an exponential growth of the oscillation amplitude; i.e. there can be an instability in which tiny oscillations (due to noise or most anything) grow until the beam hits the vacuum chamber walls (or is limited by non-linearities which is, also, usually, unacceptable since phase density has been greatly diluted).

The calculation of transverse instabilities is a complicated task, dozens of papers in the literature, with many interesting subtleties. Roughly, taking only energy spread (and not amplitude spread) into account, one obtains

$$|Z_\perp| < \frac{4mc^2}{e} \left| (n - Q)\,\eta + Q\,\xi \right| \frac{Q}{RI_0}\left(\frac{\Delta p}{mc}\right) , \qquad (8.1)$$

where n is the mode number, Q is the tune, η is the dispersion in the revolution frequency, ξ is the chromaticity, Δp is the spread in momentum, and $Z_\perp$ is the perpendicular impedance. In accord with the physical discussion given above, instability only occurs if $Z_\perp$ has an imaginary component. However, the real part of $Z_\perp$ contributes to the frequency shift of the oscillation and must be "taken care of" by the Landau damping hence it is a good approximation to have the criteria involve the absolute value of $Z_\perp$ (similar to Eq. (7.26).

Note that Eq. (8.1) only depends linearly on Δp and, roughly, is independent of energy since Δp is an adiabatic invariant. Note that unless η and ξ are of the same sign then there will be trouble at some mode number.

The transverse impedance, $Z_\perp$, can be related to the longitudinal impedance $Z_\parallel$ (Eq. 7.26 and Eq. 7.28). For a chamber of half width b, and for an oscillation of frequency ω (In Eq. 8.1) $\omega = n\,\omega_0$ where ω_0 is the revolution frequency:

$$Z_\perp = \frac{2c}{b^2}\,\frac{Z_\parallel}{\omega} \quad . \qquad (8.2)$$

For a cylindrical vacuum chamber, of radius b, containing a beam of radius a, one obtains:

$$Z_\perp = \frac{iRZ_0}{\beta^2\gamma^2}\left(\frac{1}{a^2} - \frac{1}{b^2}\right) + \frac{2cR}{\omega b^3}(1 - i)\,\rho/\delta \quad , \qquad (8.3)$$

where ρ is the resistivity of the wall (Ωm) and δ is the skin depth. This expression is only valid if the skin depth is small compared to the thickness of the vacuum chamber.

8.2 The Head-Tail Effect

The head-tail instability is a coherent instability of the transverse motion of particles in a bunch. It is driven by a coupling between the

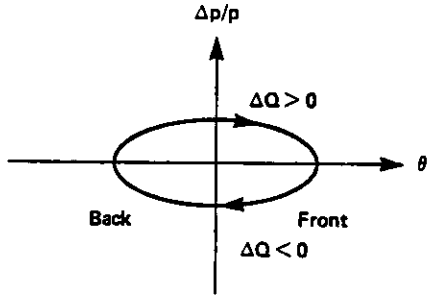

Fig. 10 A bunch showing the situation below transition ($\eta > 0$) and for positive chromaticity ($\xi > 0$).

frequency of transverse betatron oscillations and the momentum of particles; i.e. by the chromaticity. Because of this correlation, as particles move around a bunch, the phase of their betatron oscillations will change as shown in Fig. 10. One can see that the trailing particle always has the same phase shift with respect to the leading particle. This phase change is, clearly,

$$\Delta\phi = \left(\frac{\xi}{\eta}\right) Q\,\omega_0\,\tau \quad , \qquad (8.4)$$

where τ is the bunch length (in units of time).

The leading particle will, through its electromagnetic wake, effect the trailing particle. Even in the absence of resistivity, since the chromaticity creates a phase shift, the resulting motion can be unstable. Thus since the effect is present even in ideal structures it can be quite large. This is in fact the case, and after a careful study of signs one can see that if $\xi < 0$ then there can be an instability, but if $\xi > 0$ there will be no trouble (above transition). Machines "naturally" have $\xi < 0$ but modern storage rings all are made with $\xi > 0$ just to avoid the head-tail effect.

PART C: DISCRETE PARTICLE EFFECTS

IX. STATISTICAL PHENOMENA

This article quite accurately mirrors the design of an actual accelerator. Firstly, one must be concerned with the motion of single particles, as described in Part A. Secondly, one examines collective phenomena, as in Part B; here the beam moves as a fluid but the single particle motion can lead to Landau damping of the collective mode. (Other means of damping, for example by feed-back, are not covered in this article.)

Finally, one examines discrete particle effects such as radiation by particles which can, of course, be coherent (as in Free Electron Lasers), but often is incoherent. Although the phenomena of incoherent

radiation was known for a long time it was felt to be impossible to "direct each particle" which seemed to be necessary to beat Liouville's theorem (which was the basis for all the analysis of Part B). From this point of view (a very prevelant view up to 1972), stochastic cooling, the very concept and then its implementation, is quite remarkable. We shall describe the basic physics of cooling, in the last part of this section.

9.1 Radiation

An electron moving in a circular accelerator is, of course, accelerated and it will thus radiate. The amount of radiation is

$$P = \frac{2}{3}\,\frac{e^2\beta^4\gamma^4 c}{R^2} \quad . \tag{9.1}$$

Hence the radiated energy per turn is

$$\delta E = \frac{4}{3}\,\frac{\pi e^2}{R}\,\beta^3\gamma^4 \quad , \tag{9.2}$$

or, in practical units (and taking $\beta = 1$):

$$(\delta E)(\text{MeV}) = 8.85 \times 10^{-2}\,\frac{E^4(\text{GeV})}{R\ (\text{m})} \quad . \tag{9.3}$$

The radiated power, which for electrons can be very significant, is

$$P(\text{Watts}) = 10^6\ (\delta E)(\text{MeV})\ I\ (\text{A}), \tag{9.4}$$

where I is the beam current. This power loss must be made-up by the rf. In superconducting proton machines this power can be a significant source of heat at the cryogenic temperatures.

The frequency spectrum of the radiation is complicated; for low frequencies it varies as $\omega^{2/3}$. The radiation drops off exponentially for ω larger that a critical frequency, ω_c, where

$$\omega_c = \frac{3\gamma^3 c}{R} \quad . \tag{9.5}$$

Note that this frequency varies as γ^3 times the circulation frequency. Thus the radiation can extend up to very high frequencies.

The high intensity of the radiation, Eq. (9.4) and the high frequency that the radiation extends to, Eq. (9.5), is the reason for the enthusiasm for synchrotron radiation sources. Special bending magnets, wigglers, are used to make the local radius of curvature as small as possible and hence to produce intense radiation of especially high frequency.

The emission of radiation has an effect on the radiating particle. It is only for electrons that this is a significant effect, but the effect is vital in determining the property of beams in an electron

storage ring. The radiation reaction can cause either damping or undamping of the electrons' oscillations (transversely and in energy) about the equilibrium orbit. If we characterize this exponential damping rate by rate constants α_x, α_y, α_E then

$$\alpha \begin{pmatrix} x \\ y \\ E \end{pmatrix} = \frac{3\ mc^3}{e^2}\,\frac{\gamma^3}{R^2}\,J \begin{pmatrix} x \\ y \\ E \end{pmatrix} \quad , \tag{9.6}$$

where the damping partition numbers satisfy:

$$J_y = 1, \quad J_x + J_E = 3 \quad . \tag{9.7}$$

One can arrange by proper lattice design, as one must in a storage ring, to have damping in all three directions.

Thus, on the basis of the above analysis, an electron beam in a storage ring will just damp and damp so that its transverse size becomes smaller and smaller. This is approximately true, and beams become very small indeed, but they do not become arbitrarily small. Why not? Because quantum effects need to be taken into account; i.e. that electrons radiate discrete photons and that the hard photons, which are radiated statistically, kick the electron. In fact, the size of electron beams is determined by these quantum mechanical effects. The energy spread of the beam, which also damps to zero classically, is (in a uniform field).

$$\left(\frac{\sigma_E}{E}\right)^2 = \left(\frac{55}{32\sqrt{3}}\right)\left(\frac{\hbar}{mc}\right)\frac{\gamma^2}{J_E R} \quad , \tag{9.8}$$

and one can see that the finiteness of σ_E is due to a quantum mechanical effect; i.e. to the non-zero nature of Planck's constant $\hbar$. A similar formula can be given for the radial size of the beam. The vertical size is, clearly, determined by coupling to the horizontal motion.

Finally, the radiation reaction can lead to polarization of the electrons, but an exposition of this topic will not be given here.

9.2 Intra-Beam Scattering

Discrete particle effects must be invoked to understand intra-beam scattering. Generally, f course, we can ignore discrete particle phenomena, but in storage rings where particles are stored for many hours, or even days, attention must be given to even small effects.

The calculation of scattering must be done with careful attention to relativity and to small angle multiple scattering. For low-energy beams, say below 500 MeV, the scattering is important in determining equilibrium beam size (which comes into the luminosity of colliding beams or as the source size in synchrotron radiation sources).

One aspect of intra-beam scattering which is of historical interest (It was the effect which dominated the behavior of the early storage

ring ADA.) but highlights a physical phenomena, is the Touschek Effect. In the beam frame of reference, we can conveniently speak of the particles' transverse and longitudinal temperatures. It is easy to see that these are quite different with the transverse temperatures being greater than the longitudinal temperature. Intra-beam scattering, by simple thermodynamic arguments, will tend to equalize these temperatures. As a consequence the longitudinal temperature will increase and, as a result, particles will be lost from the rf bucket. That is to say, intra-beam scattering can lead to a greatly reduced beam lifetime which is the Touschek Effect.

9.3 Stochastic Cooling

Stochastic cooling is the damping of transverse and energy oscillations by means of feedback. A pickup electrode detects (say), the transverse position of an electron and send this signal, after amplification, to a kicker downstream. The time delay is such that a particle is subject to its own signal, which is done by cutting across an arc of the accelerator.

Clearly if there is only one particle this will work. Equally clearly, by Liouville's theorem, if there are many particles so that the beam can be treated as a fluid, then there will be no damping. For a finite, but very large number of particles there is a residue of the single particle effect; i.e. some damping as was first realized by van der Meer.

Consider N particles in a ring where $f = 1/T$ is the revolution frequency of particles. Suppose the electronics has a band width W. Then the pickup electrode effectively "sees" a number of particles.

$$n = \frac{N}{2WT} \quad . \tag{9.9}$$

Under the influence of the pickup and kicker this particle will have its transverse displacement, x_i, changed

$$x_i \rightarrow x_i - g \sum_{j=1}^{n} x_j \quad . \tag{9.10}$$

where g is the effective gain of the system. Consequently, the value of $(x_i)^2$ will change by:

$$\Delta(x_i^2) \equiv \left(x_i - g \sum_{j=1}^{n} x_j \right)^2 - x_i^2 \quad ,$$

$$\Delta x_i^2 = -2g\, x_i \left(\sum_{j=1}^{n} x_j \right) + g^2 \sum_{j=1}^{n} \sum_{k=1}^{n} x_j x_k \quad . \tag{9.11}$$

Initially there are no correlations between particles' positions and hence on averaging over all particles we have

$$\langle \Delta x_i^2 \rangle = -2g \langle x_i^2 \rangle + ng^2 \langle x_i^2 \rangle \quad , \tag{9.12}$$

This maximizes at $g = 1/n$ and the rate of damping of rms betatron amplitudes is

$$\frac{1}{\tau} = \frac{1}{4} \frac{1}{n} \frac{1}{T} = \frac{W}{2N} \tag{9.13}$$

where the T appears because the system works on any one particle once per turn and the factor of 4 reduction comes about from taking the rms (1/2) and the fact that phase space is two-dimensional and only x (not x') is being damped (1/2).

The assumption of no correlations is not valid, in general, and is especially complicated if one has bunches. Much of the literature is devoted to analyzing this case, which will not be discussed, here, further.

Typically, $W \sim 1$ GHz and N varies from 10^7 to 10^{12}. Thus the cooling time varies from a few milliseconds to an hour. In the Fermilab cooling ring the method, which is applied to all 3 degrees of freedom, damps (for example) the momentum space phase density by a factor of 10^4. It is this large increase in density which has made $\bar{p}$ - p colliders possible.

In the above analysis, which is, of course, very simple, we have assumed no noise in the electronics. In real life there is noise and one might think that if the amplifier noise is greater than the stochastic beam signal then there will be no cooling because the feedback system will heat the beam faster than it cools it. Not so. All one needs to do is select a lower gain and there is cooling (of course, at a reduced rate). (An analogy with a refrigerator is, perhaps, more correct.)

If there is noise, then Eq. (9.10) goes into

$$x_i \rightarrow x_i - g\left(\sum_{j=1}^{n} x_j + r \right) \quad , \tag{9.14}$$

where r is the amplifier noise expressed as apparent average x-amplitude at the pickup. The analysis now proceeds exactly as before:

$$\Delta(x_i^2) = -2g \langle x_i^2 \rangle + ng^2 \langle x_i^2 \rangle + ng^2 r^2 \tag{9.15}$$

Assuming no correlations

$$\frac{1}{\tau} = -2g + ng^2 \left(1 + \frac{r^2}{\langle x_i^2 \rangle} \right) \quad , \tag{9.16}$$

and maximizing this one obtains

$$\frac{1}{\tau} = \frac{W}{2N(1+\mathcal{N})} \quad , \tag{9.17}$$

where the factor

$$\mathcal{N} = \frac{\langle r^2 \rangle}{\langle x_i^2 \rangle} \quad ; \tag{9.18}$$

is simply noise power over signal power.

REFERENCES

1. H. Bruck, "Circular Particle Accelerators," PUF, Paris (1966). Translated by Los Alamos National Laboratory, LA-TR-72-10 Rev.
2. M. Sands, "The Physics of Electron Storage Rings, An Introduction," Stanford Linear Accelerator Center, SLAC-121 (1970).
3. "Theoretical Aspects of the Behavior of Beams in Accelerators and Storage Rings," CERN 77-13 (1977).
4. R. A. Carrigan, F. R. Huson, and M. Month, editors, "Physics of High Energy Particle Accelerators," American Institute of Physics Conference Proceedings No. 87 (1982).
5. M. Month, "Physics of High Energy Particle Accelerators," American Institute of Physics Conference Proceedings No. 105 (1983).

This work was supported by the U. S. Department of Energy under contract DE-AC03-76SF00098.

PROBLEMS

1. Employ the constancy of the Wronskian of solutions of

$$\frac{d^2 z}{ds^2} + k(s)\, z = 0 \quad ,$$

to show that the matrix in Eq. (2.7),

$$\underset{\sim}{z}(s) = M(s, s_0)\, \underset{\sim}{z}(s_0)$$

has unit determinant.

2. Show that emittance, ε, is a constant of the motion where

$$\varepsilon = \pi\, \frac{z^2 + (\alpha z + \beta z')^2}{\beta} \quad .$$

3. Derive the equations of motion for the parameters α, β, γ; namely:

$$\frac{d\beta}{ds} = -2\alpha \quad ,$$

$$\frac{d\alpha}{ds} = k\beta - \alpha \quad .$$

Show, also, that

$$z = C\, \beta^{1/2}\, e^{\pm i\phi(s)} \quad ,$$

$$\phi(s) = \int \frac{ds}{\beta(s)} \quad .$$

4. The sigma matrix formalism is often used in accelerator theory. Define a 2 x 2 matrix σ in terms of which the invariant ellipse parameters of Fig. 1 become:

$$\sqrt{\varepsilon\beta/\pi} \longrightarrow \sqrt{\sigma_{11}} \quad ,$$

$$\sqrt{\varepsilon\gamma/\pi} \longrightarrow \sqrt{\sigma_{22}} \quad ,$$

$$\sqrt{\varepsilon/\pi\beta} \longrightarrow \sqrt{\sigma_{22}\,(1 - r_{12}^2)} \quad ,$$

$$\sqrt{\varepsilon/\pi\gamma} \longrightarrow \sqrt{\sigma_{11}\,(1 - r_{12}^2)} \quad ,$$

where

$$r_{12} = \frac{\sigma_{12}}{\sqrt{\sigma_{11}\,\sigma_{22}}} \quad ,$$

$$\varepsilon = \pi \left(\sigma_{11}\,\sigma_{22} - \sigma_{12}^2\right)^{1/2} \quad .$$

Given the matrix $M(s, s_0)$, which characterizes a machine lattice (Eq. (2.7)), show that σ (at the point s) is given in terms of σ_0 (at the point s_0) by

$$\sigma = M\, \sigma_0\, M^T \quad .$$

5. Use the Hamiltonian formalism for longitudinal motion, Eq. (4.11), to evaluate the extent of the stable region in energy space; i.e. the "height of a bucket." Derive the small amplitude synchrotron frequency and, also, the synchrotron frequency as a function of synchrotron oscillation amplitude.

6. Take into account "images"; i.e. boundary conditions, using the geometry that is simplest for you, and show that the space charge limit of Eq. (5.9) has γ^3 replaced with only a γ-dependence at large γ. You will need to consider the appropriate boundary conditions for a bunched beam. (Assume the skin depth, at the bunch repetition frequency, is less than the vacuum chamber wall thickness.)

7. Work out the geometrical factor, g, in Eq. (7.12) for a cylindrical beam between conducting slabs (Eq. (7.13)) and in a cylindrical pipe where you will find

$$g = 1 + 2 \log_e (b/a)$$

8. Derive expressions for the transverse and longitudinal temperatures ($T_\perp$ and $T_\parallel$) of a beam in terms of the betatron frequency, amplitude of oscillations, etc. Make a numerical evaluation of these temperatures for some high energy machine.

LBL-18315

A Storage-Ring FEL for the VUV*

J.M. Peterson, J.J. Bisognano, A.A. Garren,
K. Halbach, K.J Kim, R.C. Sah

Lawrence Berkeley Laboratory
University of California
Berkeley, California, 94720
U.S.A.

I. Summary

A free-electron laser for the VUV operating in a storage ring requires an electron beam of high density and low energy spread and a short wavelength, narrow-gap undulator. These conditions tend to produce longitudinal and transverse beam instabilities, excessive beam growth through multiple intra-beam scattering, and a short gas-scattering lifetime. Passing the beam only occasionally through the undulator in a by-pass straight section, as proposed by Murphy and Pellegrini [1], allows operation in a high-gain, single-pass mode and a long gas-scattering lifetime. Several storage ring designs have been considered to see how best to satisfy the several requirements. Each features a by-pass, a low-emittance lattice, and built-in wigglers for enhanced damping to counteract the intra-beam scattering.

II. Introduction

The use of a "single pass", high-gain free-electron laser in a by-pass straight section of an electron storage ring has the potential of providing

* This work was supported by the Director, Office of Energy Research, Office of High Energy and Nuclear Physics, High Energy Physics Division, U.S. Dept. of Energy, under Contract No De AC03-76SF00098

coherent radiation in the VUV region with peak power on the order of tens of megawatts. Locating the FEL in a by-pass, rather than in the storage ring proper, and switching the electron beam through it only about once per damping period, has two principal advantages: It allows the use of a narrow-gap undulator without causing an unacceptabley low gas-scattering lifetime, and it allows the disruptive effects on the elctron beam produced in the high-gain FEL to be damped out in the storage ring between FEL passages, thus minimizing the effective beam emittance and maximizing the gain in the FEL.

We have considered the problem of optimizing the parameters of such a system and are reporting the progress made to date.

III. Design of the Storage Ring System

Operation of free-electron lasers in the single-pass, high-gain mode requires both high density (large peak current and small emittance) and low momentum spread. These conditions place severe demands on storage ring performance, which is limited by both coherent and incoherent multiparticle phenomena. The longitudinal microwave instability causes growth of momentum spread as peak bunch current is increased, and maximum current can also be limited by single-bunch transverse fast blow-up. Multiple intra-beam scattering can cause emittance to grow well above the natural quantum-excitation value, and single, large-angle scattering (Touschek effect) can limit beam lifetimes. The large RF systems, which are required for good Touschek lifetimes and short bunch lengths, introduce substantial impedance into the storage ring. In addition, for smooth, low-impedance beam environments, the free-space impedance at microwave frequencies is not negligible.

The heart of the matter is that the operation of a free-electron laser in the high-gain mode is essentially a controlled instability, so that beam

parameters which insure good FEL performance also make the stored beam susceptible to a variety of other instabilities. The solution to this dilemma lies on the design of the storage ring to alleviate these current limitations. Trade-offs with regard to lattice functions, synchrotron damping, RF voltages, machine radius, energy, and natural emittances can substantially improve performance.

We chose to examine two ring sizes and two beam energies and to judge these four cases on the basis of FEL performance as calculated using the FRED [2] computer program at the Lawrence Livermore National Laboratory. The storage rings considered are shown in Figures 1 and 2.

The basic lattice in each case consists of 6 achromatic sections of the Chasman-Green [3] type interspersed with three 10-meter straight sections and three damping-wiggler straight sections. Each ring has a by-pass with a 20-meter straight section for the single-pass, high-gain free-electron laser. The lattice wigglers were inserted to enhance the damping rate and thus limit the emittance growth due to multiple intra-beam scattering, as will be discussed. The 10-meter straight sections provide room for the injection system, the by-pass switches, the RF cavities, and also are available for various insertion devices.

The problem of designing suitable lattices requires obtaining low natural emittance, high momentum compaction and short damping time. The low emittance is obtained by having a sufficiently large number of achromats, in this case six. High momentum compaction, needed for longitudinal stability with small energy spread, is obtained by using long, low-field bending magnets. Since these magnets, unfortunately, produce only weak damping, it is necessary to introduce six high-field damping wigglers into the lattice.

The larger ring (150-meter circumference) has 16 quadrupoles per achromatic section and thus could be more fully optimized than the smaller ring (96-meter circumference), which has only 12 quadrupoles per achromat. The smaller ring represents an effort to mimimize the circumference.

The principal parameters of the four cases are listed in Table 1. The optics of the 500-MeV and 750-MeV versions of each ring differ principally because in each case the wiggler peak magnetic field was set at 1.8 telsa. Mechanically the rings are very close. The lattice functions for cases A and B are illustrated in Figure 3.

IV. High Intensity Effects

Since good FEL operation is based on a controlled beam instability, it is not surprising that other, more deleterious high-intensity effects can also occur in this high-beam-density domain. The most serious of these effects are the longitudinal and transverse coherent instabilities and multiple intra-beam scattering.

A. Coherent Beam Instabilities and Impedance

The threshold peak current for the longitudinal microwave instability is given by:

$$I_p^L = \frac{2\pi\alpha\,(E/e)\sigma_p^{\,2}}{Z_n/n} \qquad \text{(amperes)} \qquad (1)$$

where α is the momentum compaction factor, E is the beam energy (in eV), σ_p is the rms fractional momentum spread, and Z_n is the longitudinal coupling impedance (ohms) at the nth harmonic, here evaluated at the frequency $\omega = \sigma_s/c$ for the rms bunch length σ_s.

The threshold for the transverse instability is:

$$I_p^L = \frac{4\pi\sqrt{2}E\nu_s}{eZ_t\bar{\beta}}\,F(b/\sigma_s) \qquad (2)$$

where ν_s is the synchrotron tune, Z_t is the effective transverse impedance, $\bar{\beta}$ is the average value of the beta function in the transverse plane under consideration, b is the radius of the vacuum pipe, and F is a form factor of the order of unity.

For the examples considered here, the longitudinal instability produces the more stringent limit. We note that a larger compaction factor provides a larger longitudinal threshold. However it will develop that a larger compaction factor tends also to produce a larger emittance growth from multiple intra-beam scattering. Thus the choice of optimum compaction factor is somewhat complicated.

The sources of longitudinal coupling impedance include beam-pipe discontinuities, the RF cavities, and the free-space impedance at frequencies well above the beam-pipe cut-off. For this study 1 ohm was allotted for vacuum chamber discontinuities. An additional 1 to 3 ohms was introduced in the peak Z_n/n by the RF system, which was sized to produce a momentum dynamic aperture of ±3 percent, so as to provide an adequate lifetime for large-angle intra-beam scattering (Touschek effect).

From experience at SPEAR it is expected that above the pipe cut-off Z_n/n will fall as $(\omega_c/\omega)^{1.7}$. From this scaling, at frequencies corresponding to a bunch length of about 1 cm, the effective Z_n/n is less than 1 ohm for the combination of vacuum-chamber discontinuities and RF system.

The peak value of the free space impedance is given by the approximate relation:

$$\left(\frac{Zn}{n}\right)_{freespace} = 300\frac{b}{R} \text{ ohms} \qquad (3)$$

This value of impedance appears at frequencies well above pipe cut-off, where shielding of the synchrotron radiation process disappears.

If wigglers are introduced for enhanced synchrotron-radiation damping, there is an additional contribution proportional to the total additional absolute angular bend in the wigglers. Values in the 1 ohm range were obtained for the smaller rings considered.

B. Multiple Intra-Beam Scattering

Multiple Coulomb scattering between electrons within a bunch can lead to excitation of betatron oscillations and energy spread. If the synchrotron damping is weak compared with the diffusion rate induced by this intra-beam scattering, the equilibrium beam emittance can be substantially larger than the natural quantum emittance.

The theory of intra-beam scattering has been developed most fully in the work of Piwinski [4] and that of Bjorken and Mtingwa [5]. The detailed formulation requires numerical evaluation of rather involved expressions for transverse and longitudinal diffusion rates. The basic mechanism can be summarized as follows: In a typical intra-beam scattering event some transverse momentum is converted to longitudinal. This increase in longitudinal momentum coupled with the local dispersion function can increase the horizontal emittance in the same way that it tends to be increased by quantum excitation.

For electron storage rings of interest here there is growth in both longitudinal and horizontal emittance, and the primary scattering is from horizontal into longitudinal. An equilibrium emittance is reached when the intra-beam and quantum-exitation diffusion rates are balanced by the horizontal synchrotron damping. This condition is summarized by:

$$-g\epsilon_H + g\epsilon_o + G(\epsilon_H)\epsilon_H = 0 \qquad (4)$$

where g is the synchrotron damping rate, ϵ_H is the horizontal emittance, ϵ_o is the nominal quantum-exitation emittance, and $G(\epsilon_H)$ is the intra-beam-scattering diffusion rate, which is a complicated function of ϵ_H. In the parameter regime of interest, however, it is found that $G(\epsilon_H)$ is proportional to $(\epsilon_H)^{-2}$. Let $\hat{\epsilon}$ be the value of ϵ_H where $G(\hat{\epsilon})$ equals g -- that is, where the synchrotron damping equals the intra-beam diffusion rate. Then it follows from equation (4) that the equilibrium ϵ_H is given by:

$$\epsilon_H = \frac{1}{2}\left[\epsilon_o + (\epsilon_o + 4\hat{\epsilon}^2)^{1/2}\right] \qquad (5)$$

The scaling of this equilibrium emittance is not clear cut because the basic relations are not simple functions. It has been found useful to vary the relevant parameters in numerical evaluations to yield local behavior. For the lattices considered in this study, it was found that the growth rate of the horizontal emittance was proportional to the average value of the quantity

$$\left\langle \frac{I_p \tilde{\mathcal{D}}}{\epsilon^2 \beta_y^{1/3} \sigma_p \gamma^3} \right\rangle \qquad (6)$$

where I_p is the peak beam current, $\tilde{\mathcal{D}}^2 = \mathcal{D}^2 + (\alpha\mathcal{D} + \beta\mathcal{D}')^2$, D being the dispersion

function, D' its slope, α and β the usual horizontal betatron functions, β_y the vertical betatron function, σ_p the rms fractional momentum spread, and γ the electron energy in units of the electron rest mass.

Using this proportionality, equation (5) can be rewritten as

$$\epsilon_H = \frac{1}{2}\left[\epsilon_0 + \left[\epsilon_0^2 + (\text{const})\left(\frac{I_p \bar{D} \mathcal{T}_s}{\beta_y^{1/3}\sigma_p \gamma^3}\right)\right]^{1/2}\right] \qquad (7)$$

where $\mathcal{T}_s$ is the synchrotron damping time. The constant is determined by the numerical evaluation of a particular case. Thus from an intra-beam-scattering point of view, design goals include: small natural emittance, small dispersion, small damping time, large β_y in the dispersion region, large σ_p, and high energy. Unfortunately, not all these conditions are consistent with other storage-ring current limitations or with optimum FEL performance. In particular, as was noted earlier, smaller dispersion results in a smaller compaction factor, which reduces the microwave instability threshold.

IV. Operating Conditions

Choice of the optimum operating conditions of a storage ring for FEL operation is complicated by the interdependence of the operating parameters at high beam intensities. Larger momentum spread allows larger currents through the microwave instability but tends to degrade FEL performance. Larger currents tend to produce larger emittance through intra-beam scattering, so that whether the current density also increases is not immediately apparent.

Our first step toward finding the optimum ring and its optimum operating conditions has been to consider for each ring two energies (500 and 750 MeV), two values of momentum spread (.001 and .002), and two values of vertical-to-horizontal emittance coupling ratio (1/10 and 1/1)-- a total of 16 cases. From these parameters are derived the corresponding values of maximum beam

current, emittance, and RF voltage. Table 2 shows the operating conditions for 8 of the cases considered.

V. FEL Performance

The FEL performance for each of the 16 cases was judged both by analytical expressions derived from theory [1,6-14] and by the results of the two-dimensional simulation code FRED.

One-dimensional theory predicts exponential growth and a saturation power level. The e-folding length for growth of the radiation power is

$$l_e = \frac{\lambda_w}{8\pi\rho\, f(\sigma_p/p)} \qquad (8)$$

where λ_w is the wiggler period, ρ is the FEL gain parameter, which for a planar undulator is approximately

$$\rho = \left\{\frac{K^2}{16\pi}[J_0(\mu) - J_1(\mu)]^2 \lambda_w^2 n_e r_e / \gamma^3\right\}^{1/3} \qquad (9)$$

where K is the rms undulator parameter = $0.934\lambda_w(\text{cm})B(T)$, B the rms wiggler field strength, n_e the volume density of the electron beam, r_e the classical electron radius, $\mu = K^2/(1 + K^2)$, and $f(\sigma_p/\rho)$ is a function of the electron fractional energy spread in units of ρ; the value f(0) is 0.866, and f(1) is 0.31 for a Lorentzian momentum distribution. Note that equations (8) and (9) are generalized relative to those of reference [1] in that they apply to a planar undulator and include the effects of momentum spread.

B for a hybrid wiggler using samarium-cobalt permanent magnets (B_r = 0.9 Telsa) is approximately [15]

$$B = 2.36\, e^{-g/\lambda_w(5.47 - 1.8g/\lambda_w)} \quad \text{(Tesla)} \qquad (10)$$

where g is the wiggler full gap. The wiggler period and the radiation wave length λ are related by the resonance condition

$$\lambda = \frac{\lambda_w}{2\gamma^2}(1 + K^2) \qquad (10)$$

The exponential growth of the radiation field eventually levels off. The saturation level is expected to be of the order of ρE_b, E_b being the power in the electron beam. The number of undulator periods need to reach saturation is expected to be about $1/\rho$; thus the undulator length required to reach saturation is approximately λ_w/ρ.

The FEL parameters and estimated operating levels are listed in Table 2. Comparison of these operating levels with those computed by the two-dimensional simulation code FRED has started but as yet is far from complete. The preliminary results seem to indicate qualitative agreement -- i.e., the cases which look better on the basis of analytic expressions also look better according to FRED. Quantitatively, the results at present are not conclusive The exponentiating length according to FRED is typically about 50 percent longer than the analytic estimate, and the saturating power level is typically an order of magnitude lower. Sometimes the agreement is better and sometimes worse. The systematics of the quantitative differences are not yet understood, but there are indications that diffraction effects are at least partly responsible.

VI. Conclusions

In comparing the various rings and operating conditions, the present results indicate that the 150-meter ring operating at 750 MeV with a σ_p of .002 and an emittance-coupling ratio of 0.1 is the best of the 16 cases considered. Whether a larger radius ring is significantly better

yet clear, because in the light of these studies we can now see the possibility that the lattice of the smaller ring could be significantly improved with respect to both natural emittance and intra-beam scattering.

The power levels available from a high-gain FEL may not be as high as anticipated on the basis of analytic theory, but nevertheless the computational results indicate that powers on the order of tens of megawatts can be obtained in systems like those considered in this report.

Table 1

The Principal Lattice Parameters of the Four Rings Considered

CASE	A	B	C	D
Circumference, m	150	96	150	96
Beam energy, MeV	500	500	750	750
Superperiods	3	3	3	3
Insertion SS, m	10	10	10	10
Wiggler SS, m	9	5.4	9	5.4
Bend field, T	0.218	0.647	0.327	0.873
Wiggler field, T	1.8	1.8	1.8	1.8
Wiggler length, m	3 x 7.8	3 x 4.2	3 x 7.8	3 x 4.2
Wiggler period, m	0.3	0.3	0.3	0.3
Betatron tunes, x/y	6.68/7.72	5.31/5.27	6.63/6.60	6.69/3.44
β in SS, x/y, m	2.8/5.0	10/3.2	3.2/4.6	3.0/7.0
Chromaticity x/y	15.0/17.7	11.0/10.6	13.7/12.0	23.5/7.1
Compaction factor α	.0166	.0074	.0167	.0084
τ_x without wigglers, sec.	0.69	.15	.21	.05
τ_x with wigglers, sec.	0.030	.030	.019	.016
ϵ_{xo}, natural, 10^{-8} rad-m	0.246	0.654	0.324	0.834
σ_p, natural, without wigglers, 10^{-4}	1.55	2.67	2.33	3.80
σ_p, natural, with wigglers, 10^{-4}	4.36	4.16	5.24	4.97

Table 2

8 Sets of Operating Conditions

Ring circumference, m	150	96	150	96	150	96	150	96
Beam Energy, MeV	500	500	750	750	500	500	750	750
Momentum spread σ_p	.001	.001	.001	.001	.002	.002	.002	.002
ϵ_y/ϵ_x	0.1	0.1	0.1	0.1	0.1	0.1	0.1	0.1
ϵ_x, 10^{-8} rad-m	1.23	0.98	0.71	0.84	1.74	1.27	0.96	0.93
σ_s, cm	1.25	1.25	1.25	1.25	1.25	1.25	1.25	1.25
Peak current, amp	74	23	82	46	296	93	327	183
$RF_{voltage}$, MV	3.0	0.86	4.5	1.5	3.0	0.86	4.5	1.5
FEL parameters:								
λ, A°	400	400	400	400	400	400	400	400
λ_w, cm	1.88	1.88	2.34	2.34	1.88	1.88	2.34	2.34
K (rms)	1.80	1.80	2.58	2.58	1.80	1.80	2.58	2.58
Gain parameter, ρ, 10^{-3}	1.13	0.83	1.22	0.95	1.60	1.21	1.75	1.46
ρE_b, MW	42	9.5	75	33	237	56	429	200
λ_w/ρ, m	16.6	22.7	19.2	24.6	11.8	15.5	13.4	16.0

[1] J.B. Murphy C. Pellegrini, "Generation of High Intensity Coherent Radiation in Soft X-Ray and VUV Region", BNL unpublished, 1984.

[2] Access to the FRED program was generously provided by Andrew Sessler, Donald Prosnitz, and Ernst T. Scharlemann.

[3] R. Chasman and G.K. Green, BNL 50595 (J.P. Blewett editor), Vol. 1, pp 4-4 to 4-8, 1977.

[4] Piwinski, "Intra-Beam Scattering", IXth International Conference on High Energy Accelerators, SLAC, 1974.

[5] J. Bjorken and S. Mtingwa, "Intra-Beam Scattering", Particle Accelerators, 13, 115, 1983.

[6] R. Bonifacio, L. Narducci, and C. Pellegrini, "Proc. of Topical Meeting on Free Electron Generation of Extreme UV Coherent Radiation, BNL, Sept 1983, AIP Conf. Proc. No. 118, Subseries on Optical and Engineering No. 4, 1984.

[7] N.M. Kroll and W.A. McMullin, Phys. Rev. A17, 300 (1978)

[8] A. Gover and Z. Livni, Opt. Comm. 26, 375 (1978).

[9] I.B. Bernstein and J.L. Hirshfeld , Phys. Rev. A20, 1661 (1979).

[10] C.C. Shil and A. Yariv, IEEE J. of Quantum Electron., QE-17 1387 (1981).

[11] P. Sprangle, C.M. Tang and W.M. Manheimer, Phys. Rev. A20, 302, (1980).

[12] G. Dattoli, A. Marino, A. Renieri, F. Romanelli, IEEE J. of Quantum Electron. , QE-17, 1371 (1981).

[13] A. Gover, P Sprangle, IEEE J. of Quantum Electron. , QE-17, 1196 (1981).

[14] R. Bonifacio, F. Casagrande and G. Casati, Opt. Comm. 40, 219 (1982).

[15] K. Halbach, Journal de Physique Collogue C1-211, Tome 44 (1983)

List of Figures

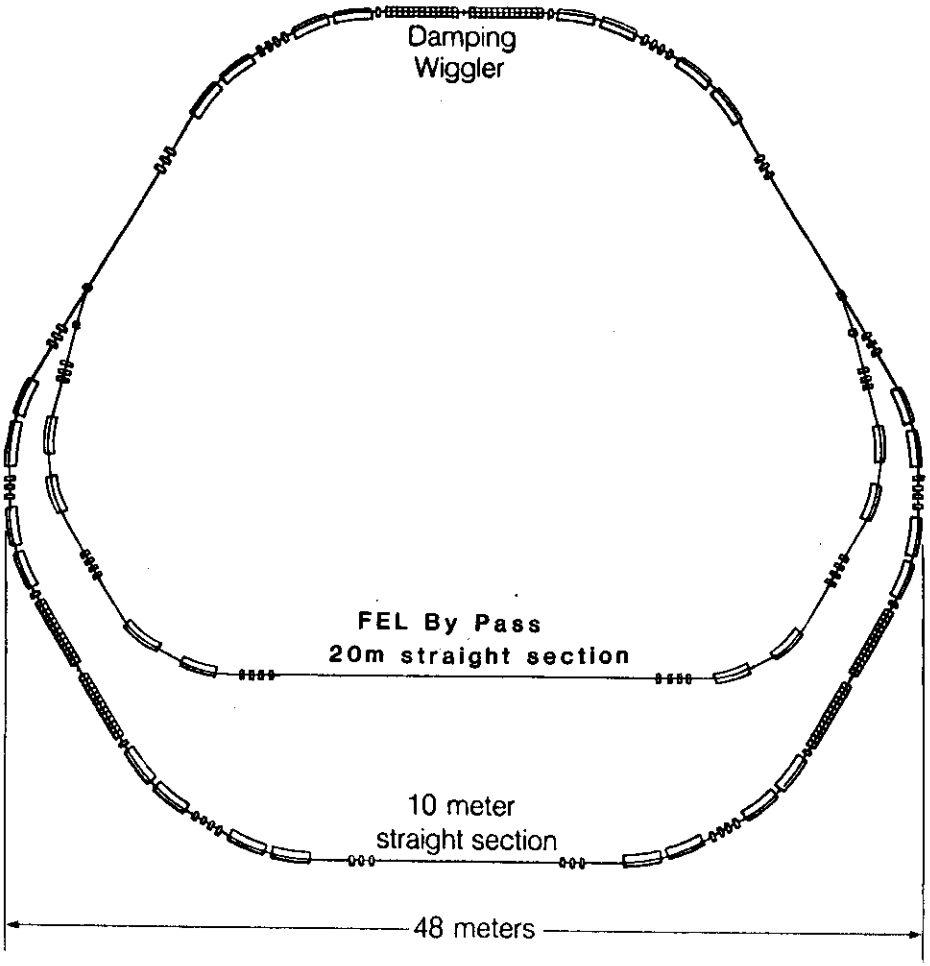

Figure 1 150 meter Circumference Storage Ring with FEL By-Pass

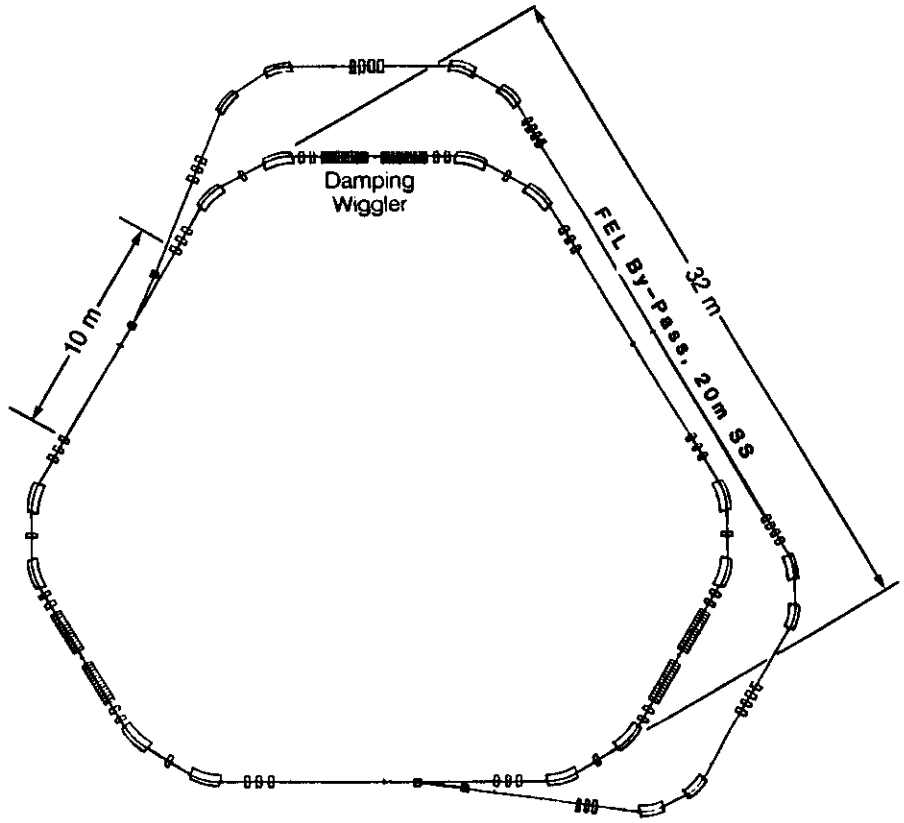

Figure 2 96 meter Circumference Storage Ring with FEL By-Pass

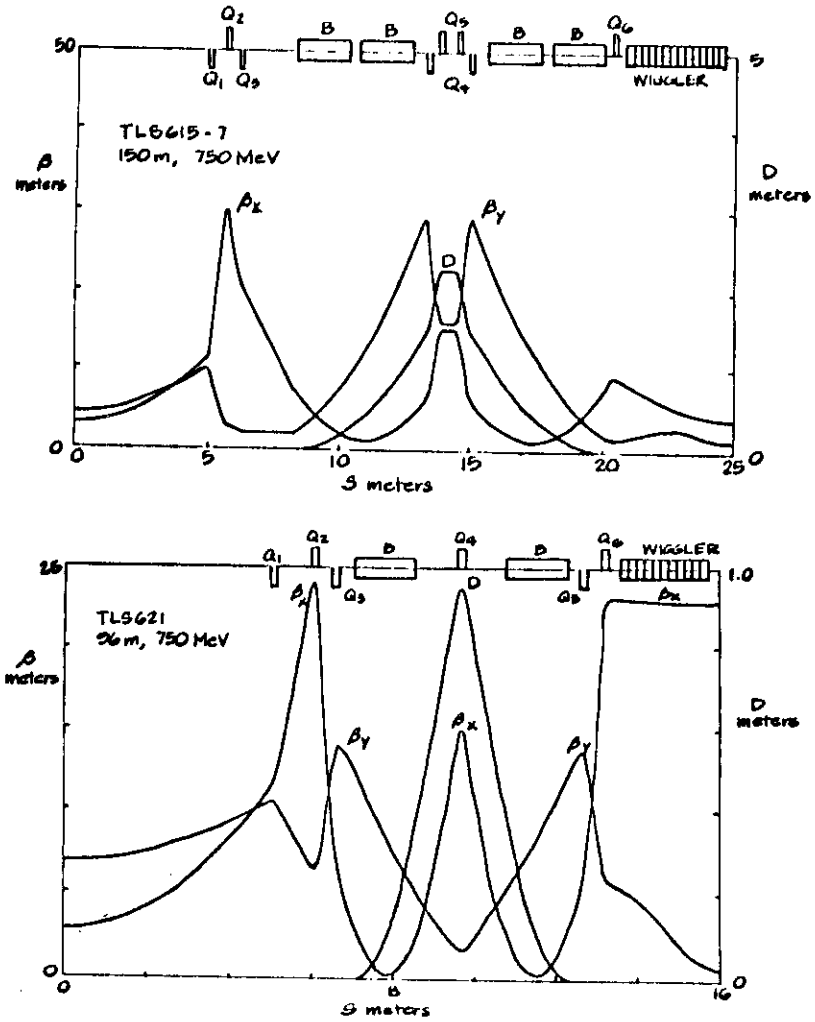

Figure 3 The betaron and disperion functions for the 150-meter and the 96-meter lattices at 750 MeV.